SPHERICAL ELECTRIC MOTOR DESIGN

A Dissertation by

Atilla Akil

Master of Science, Wichita State University, 2005

Bachelor of Science, Hacettepe University, 1993

Submitted to the Department of Electrical Engineering and Computer Science
and the faculty of the Graduate School of
Wichita State University
in partial fulfillment of
the requirements for the degree of
Doctor of Philosophy

May 2013

SPHERICAL ELECTRIC MOTOR DESIGN

The following faculty members have examined the final copy of this dissertation for form and content, and recommended that it be accepted in partial fulfillment of the requirements for the degree of Doctor of Philosophy with a major in Electrical Engineering.

_____
John M. Watkins, Committee Chair

_____
Mahmoud E. Sawan, Committee Member

_____
Ward T. Jewell, Committee Member

_____
Gamal Weheba, Committee Member

_____
Rena Hixon, Committee Member

Accepted for the College of Engineering

_____
Vish Prasad, Dean

Accepted for the Graduate School

_____
Abu S. M. Masud, Dean

DEDICATION

To my father who passed away suddenly during this research

I hear and I forget. I see and I remember. I do and I understand.

—Confucius (*Chinese philosopher & reformer (551 BC– 479 BC))*

ACKNOWLEDGMENTS

During this research and the writing of this dissertation, I have always felt great support and motivation by many people. I would like to extend my sincere appreciation to my advisor, Professor Emeritus M. E. Sawan. Without his comprehensive advice, it would not have been possible to complete this research and to be confidently ready for the next challenges ahead of me in my life. I would also like to extend my sincere appreciation to my committee chair, Professor J. M. Watkins. His important suggestions and warm support have always been very helpful and motivating.

I extend my sincere appreciation to Professors W. Jewell and R. Hixon for their warm support and motivation. I also extend my sincere gratitude to Professor Gamal Weheba, who helped me to build the main frame of this prototype in his laboratory. He has always given me invaluable advice.

My sincere appreciation goes to my previous employer, Dr. Sophokles Anthimides, and Trees For Life, Inc., where I did my internship during my master's studies.

Especially, I thank my family. Their unlimited support and love have been the main encouragement in my studies.

Thank you all very much.

ABSTRACT

To date, electric motors have been rotary and linear with one degree of freedom (DOF) motion. Advancements in technology have brought new, complex machines requiring multiple degrees of freedom motion; however, this is currently being provided by connecting single-DOF motors together, such as in a robotic ankle joint, where three servo motors are combined and 3-DOF motion are obtained. However, the end-product is heavy, complex, and inefficient in many ways. Several researchers have been studying spherical motors in order to obtain a 3-DOF motion motor. The first attempt was in 1959 by Williams et al. [1]. Then other researchers began investigating 3-DOF motion using a single actuator. Unfortunately, a spherical electric motor (SEM) has not been commercialized yet because of some difficulties in realizing 3-DOF with a single motor. Position resolution accuracy is very difficult to achieve in an SEM, and the bearing system is another challenge. Transfer and magnetic bearings have been introduced as the solution; however, under high torque, transfer bearings create high friction, and magnetic bearings cannot handle the load. The actuation method remains the biggest challenge in developing an SEM. In this research, the goal was to develop an SEM that could be applied to industry relatively soon. First, a new actuation method was introduced by concentrating on position accuracy. Similar methods have been used in liquid crystal display (LCD) and magnetic suspension systems, whereby an array of coils on the stator surface are controlled to create a moving stator pole coupled with a rotor pole that moves together, thus realizing 3-DOF. Second, an electromagnetic torque model was derived for an SEM. Finally, a dynamic model was developed, and a dynamic decoupling control system was designed. Results show that position accuracy was achieved reasonably because the torque model is promising for calculating the required currents based on torque values calculated by the computed torque model.

TABLE OF CONTENTS

TABLE OF CONTENTS (continued)

LIST OF FIGURES

ABBREVIATIONS

AC	Alternate Current
CTM	Computed Torque Control
DC	Direct Current
DDCTM	Dynamic Decoupling Computed Torque Model
DOF	Degree(s) of Freedom
LCD	Liquid Crystal Display
Maglev	Magnetic Levitation
MMF	Magneto Motive Force
PID	Proportional Integral Derivative
PD	Proportional Derivative
PD+	Proportional Derivative Plus
SEM	Spherical Electric Motor

NOMENCLATURE/SYMBOLS

α	Alpha, latitude of stator coil, rad
β	Beta, longitude of stator coil, rad
ϕ	Phi, pitch angle (about x axis) of the rotor shaft, rad
θ	Theta, yaw angle (about y axis) of the rotor shaft, rad
ψ	Psi, roll angle (about z axis) of the rotor shaft, rad
δ	Delta, separation angle for stator coil from edge of rotor pole, rad
ω	Omegas, angular velocity for pitch, yaw, and roll, rad/s
μ	Mu, permeability, kg m /s^2 A^2
Φ	Phi, magnetic flux, Weber
I	Current, A
v	Voltage, volt
N	Number of turns in stator coils
n	Number of coils on stator
B	Magnetic flux density, T
H	Magnetic field strength, A/m

CHAPTER 1

INTRODUCTION

Using electromagnetic force, electric motors convert electrical energy into mechanical energy. An electric motor can be either rotary or linear in style. Both of them provide a single degree of freedom (DOF). If multiple degrees of freedom are required, then a greater number of electric motors should be used.

Rotary motors are used in those machines that need rotation, such as robots, fans, and electric cars. In a robot, for example, an electric motor is used for the joints. As is known, most robotic joints are required to have multiple DOF. Therefore, multiple electric motors are installed in a single joint. A person sitting in the corner of a room could not request more wind from a ceiling fan because the fan would not be able to tilt without an additional motor being used. Moreover, one could not steer an electric car by using the same motor that is used for wheel rotation; for that, an additional motor is needed.

Linear motors are used in machines that need straight-line force such as in power door lock actuators in cars and magnetic levitation (maglev) trains. A power door lock actuator can only lock and unlock a door, not enable or disable child safety mechanisms, for example, without an additional actuator. The maglev train cannot be elevated or lowered as it is moving because the linear motor has only one DOF.

In industry, rotary electric motors are used for more than just linear applications. Therefore, this research aimed to improve on rotary motors, more specifically, to design a single rotary motor with multiple degrees of freedom.

1.1 Motivation

Can a single special motor have multiple DOF? In this research, the possibility of creating an electric motor with multiple DOF was investigated.

1.1.1 Spherical Electrical Motor

A motor that operates about all three axes has three DOF: roll, pitch, and yaw. Considering a ball joint, which has three DOF, helps one understand the dynamics of multi-DOF motion, even though the ball joint is not an actuator. If there is any way to actuate a ball joint, then the new device would be called a spherical electric motor (SEM).

Traditionally, a possible SEM would have a rotor and a stator as its main parts. However, both would have to be globular, so the motor could provide multiple degrees of freedom.

1.1.2 Applications

In the design of an ankle joint in a humanoid robot, three servo motors have been used to offer three DOF. This was a difficult and inefficient design for several reasons, among them a complicated control algorithm, large space requirements, high cost, and reliability problems. A new special motor providing three DOF may be used as a joint in humanoid robots. Such spherical actuators can also be used in electric car wheels and air vehicle propulsion systems.

Since motors in use today provide only one degree of freedom, one SEM may replace several motors that are used in devices designed to provide multiple DOF.

1.2. Objective

Typically, electric motors provide only a single degree of freedom, so in complex machines where more DOF are needed, the number of motors must be increased. Consequently, these machines become more complex and inefficient. For example, in many recent applications, robots have been used with high efficiency. In many cases, robotic joints have multiple DOF.

Instead of using multiple motors in robotic joints, one motor with multiple DOF could be used. Actually, a well-design SEM could perform better then multiple motors.

Several researchers with a similar idea have attempted to build an SEM by using different methods, but these have not been applied in industry. One of the goals of this research is to develop an SEM that can be industry applicable. Therefore, it is important to consider its functionality, simplicity, and reliability. The actuation method, bearing system, and material selection are important aspects of this research.

Unfortunately, there is currently no SEM in use in industry, even though there have been different theoretical approaches. More investigation with positive results is needed for industrial applications using an SEM. If expected industrial functionality of an SEM is attained, then a large portion of the goal can be considered achieved. Simplicity is another important step in industrial applications. Naturally, sophisticated yet simple devices are generally attractive to societies for many reasons: low cost, user friendliness, and easiness to maintain. Certainly reliability should be a reasonable reason for a device to be used in industrial applications. Testing should be done in a comprehensive way in order to validate the robust system.

In this research, the actuation method was the main area of investigation. The method proposed herein is a new approach for actuation of a spherical electric motor to use in industrial applications. Certainly, other aspects can be investigated in future research. The magnetic bearing system is important for an efficient SEM since the rotor is moving in three axes. Material investigation is also important due to the wide area of usage and magnetic field properties. An SEM can be used anywhere—from food plant robots to space robots, to submarine robots, to implant joints—so the material used in an SEM needs to have flexible peculiarities for different application areas. The main objective of this research was to design a less-complex, versatile,

and inexpensive electric motor with three DOF. In this dissertation, an SEM has been studied, considering all aspects of its real application.

1.3. Contribution

The expected contribution of this research is using the SEM in industrial applications to develop less-complex, more-versatile, and affordable products for the public. An electric motor along with its control system is a major part of most devices. Improvements in electric motors and their control systems would make a large impact on societies.

1.4 Structure of the Dissertation

Chapter 2 presents a literature survey, as well as a review of electromagnetism and its application in electric motors. Electric motors and their principles will be studied as well. In Chapter 3, a spherical electric motor will be studied in detail. The actuation method, working principles, and structure of an SEM will be described. In Chapter 4, magnetic field and torque modeling will be investigated. In Chapter 5, kinematics and dynamics of the system will be presented. In Chapter 6, a closed-loop controller for an SEM will be designed and tested. Finally, in Chapter 7, a conclusion will be reached.

CHAPTER 2

TECHNICAL BACKGROUND

In this chapter, the previous research work for a spherical electric motor and SEM control systems will be presented. Then the principles of electric motors will be discussed briefly, followed by the types of electric motors.

2.1 Literature Survey

Research on an SEM is an uncommon subject due to its complexity and cost [2]. Electromechanical design and control system are the main areas that SEM researchers have studied.

2.1.1 SEM

According to a Web search, the first SEM was introduced by Williams et al. [1]. However, their goal was to adjust the speed by rotating the stator. Both stator and rotor were spherical, but the output shaft had only one degree of freedom.

Spherical Induction Motor

In 1986, Davey and Vachtsevanos [2] and Davey et al. [3] introduced an SEM with multiple DOF. Speed, position, and torque controls of the SEM were their goals. Their induction motor, like actuation methodology, was never applied in industry [4].

Spherical DC Servo Motor

Kaneko et al. designed a spherical DC servo motor [5]. The rotor was supported by a gimbal mechanism with encoders. The stator was spherical and had three windings. The disk-like rotor had four permanent magnet poles.

Spherical Stepper Motor

In a spherical stepper motor, the rotor has a permanent magnet or soft iron poles embedded at the equator, and a spherical stator that has two layers of poles, one in the south and one in the north. Based on the desired position of the shaft, either the upper or lower pole of the stator is energized, thus causing the shaft to tilt. If both the south and north layers of the coils are energized, then the rotor rotates on its own axis. This method is not in use today. Position resolution accuracy is very low in this method, and in robots, for example, this is very important. With a closed-loop servo controller, the shaft position error can be minimized; however, most likely, oscillation would occur. The mechanical complexity of the spherical stepper motor has led researchers to explore different methods.

Lee and Kwan introduced another actuation method for a spherical electric motor [6]. Their method was to use variable reluctance motor principles in an SEM, whereby attraction between stator coils and rotor poles would create torque and cause the rotor to rotate. According to the published research, this method has not yet been applied in industry.

Chirikjian and Stein, of Johns Hopkins University, designed a "spherical stepper motor" [7]. The varying number of poles in a spherical rotor and spherical stator prevents motion singularity. One or more pairs of rotors and stator poles interact, thus causing rotor movement. In other words, this method is very similar to that of conventional rotary stepper motors. It has been more than a decade since this motor was designed, and it is not in use yet. In this method, it is very difficult to achieve position accuracy due to the spherical motion. If the poles are built in a smaller size (to increase accuracy by decreasing step angle), then magnetic flux becomes insufficient to create enough force.

About three decade of spherical motor research in either induction or stepper motor developments [8-10] passed before a new method [11] was introduced [12, 13].

Spherical Ultrasonic Motor

Toyama et al. introduced a spherical ultrasonic motor consisting of three stators and an inner rotor [11]. This team worked on two different methods: stationary wave and traveling wave. They have continuously produced several SEMs using similar methods in their laboratory at Tokyo University of Agriculture and Technology. Other researchers have worked on the spherical ultrasonic motor [14].

As shown above, methods have been implemented in theoretical and applied research to attain some positive results toward multi-DOF motion. The main goal was to have multi-DOF motion that could be controlled with reasonable accuracy. During the literature survey, no publication about commercialization of the above methods was revealed.

2.1.2 Control Systems for SEM

Conventional motors with one degree of freedom were previously used with heavy, costly, and inefficient mechanical transmissions to adjust torque, speed, and position. With newer technology has come alternate current (AC) and direct current (DC) motor drives, which are better able to adjust torque, speed, and position.

For a spherical electric motor, having a drive makes more sense than the conventional 1-DOF motor due to the SEM's complexity. Control system design is the main work in a drive. Therefore, a literature survey for the control system is presented in this separate section.

Spherical Induction Motor Control System

Davey and Vachtsevanos introduced input voltage and stator frequency control for a desired rotor speed in their SEM [2]. They also showed that efficient torque production is still possible with continuous speed control [3].

Spherical DC Servo Motor Control System

Kaneko et al. designed a dynamic controller for a spherical DC servo motor [5].

Spherical Stepper Motor Control System

Qian et al. introduced complete dynamic modeling and a proportional derivative (PD) controller design for a spherical stepper motor [15]. They had positive results for prevention of motion singularities. Wu et al. presented an open-loop controller for a spherical stepper motor [16]. Their torque modeling was based on the Lorentz force law. The linear relationship between the Lorentz force law and input current was advantageous.

Due to the nature of the stepper SEM, a sophisticated control scheme is required [6, 9]. Researchers have studied different approaches toward control of the stepper SEM. One of the reasons for the complexity of the stepper SEM is the multiple coils. Forward dynamics has provided a unique solution, but inverse dynamics has infinite solutions due to multiple coils. Therefore, in addition to solving the forward dynamics, the optimization problem for the input vector must be solved [9].

In a stepper SEM, another complexity issue is with the bearing system. Conventional 1-DOF motors have regular ball bearings on each side of the motor; however, in an SEM, since the rotor is moving in three dimensions, the conventional bearing system cannot be applied. Zhou and Lee introduced a reaction-free control scheme based on magnetic levitation [10]. Also, Ezenekwe and Lee designed an air bearing system for the stepper SEM [13].

Position detection is also complicated in SEMs due to the three-dimensional motions. In earlier research, two encoders 90 degrees apart from each other were used [5, 6, and 9]. Later on, a machine vision-based method was applied [17, 18].

In summary, the stepper SEM control system research was broadly performed for torque modeling and a dynamic system for an SEM [19–27].

Spherical Ultrasonic Motor Control System

Stationary and traveling waves are the main methods of spherical ultrasonic motors. Using the Hall element for position detection and magnetized rotor, Purwanto and Toyama introduced a proportional integral derivative (PID) controller for a spherical ultrasonic motor [14]. The control was for one degree of freedom only, and noise was ignored. Ishikawa and Kinouchi introduced a nonlinear control based on nonholonomic mechanics for a spherical ultrasonic motor [28].

Many different approaches have been explored in control systems research for SEMs. Dynamic system simulations have been done using different algorithms like the PD, PD+, and dynamic decoupling based on the computed torque model [29–50]. A common goal of all of this research was robust torque and dynamic modeling, so desired speed, torque, and position could be achieved by the proposed controllers. Some of them had good results toward precise motion control; however, according to published research, they have not yet been commercialized.

Both the SEM and its drive systems have been studied for about half a century. Induction, stepper, and ultrasonic actuation methods have also been studied, and varieties of control systems have been applied in the SEM. However, according to published research [51–54], none of this is ready for industry applications.

2.2 Electric Motor Principles

This section presents the basic principles of electric motors and related techniques, which will lay a good foundation for the remainder of this document.

2.2.1 Vectors and Fields

Vectors

In engineering, the three main steps to studying any system are modeling, design, and analysis. During modeling, all parameters must be considered. These parameters could be temperature, distance, dimensions, or velocity. For example, an electric motor can have 100 mm length and 50 mm outside diameter. This information would be technically enough. However, when velocity is considered, magnitude would not be enough to describe it. Direction of the velocity is also needed. A quantity like velocity, which is specified by magnitude and direction, is called a vector. A quantity like temperature, which is specified by magnitude, is called a scalar.

Fields

A single vector represents the quantity for a certain time and position. The speed of an electric motor might vary based on the time and position. The speed vector is a single quantity, whereas the speed vector field is dissemination of the speed vector in time and position.

2.2.2 Electromagnetism

The smallest component of a regular substance is the atom. Protons (positively charged) and neutrons are located within the nucleus of an atom, which is surrounded by electrons (negatively charged). According to Coulomb's law, an electric charge is created by protons and electrons, and the unit for the charge is Coulomb (C).

One Coulomb per second provides the electric current, the unit of which is ampere (C/s = A). By the Lorentz force law, the magnetic field (B) is generated by an electric current (I). The unit for the magnetic field is tesla (T). The magnetic field direction can be determined by the right-hand rule. In a wire with length L, when current (I) is applied, the resultant electromagnetic force (F) is given by

$$\vec{F} = \vec{I}L \, x \, \vec{B}$$

2.2.3 Motion Production

In an electric motor, regardless of its type, the general principle is magnetic attraction and repulsion. Figure 1 shows the general principle of electric motors. The rotor and stator may have multiple poles, and the interaction between the rotor and stator poles causes rotation of the rotor.

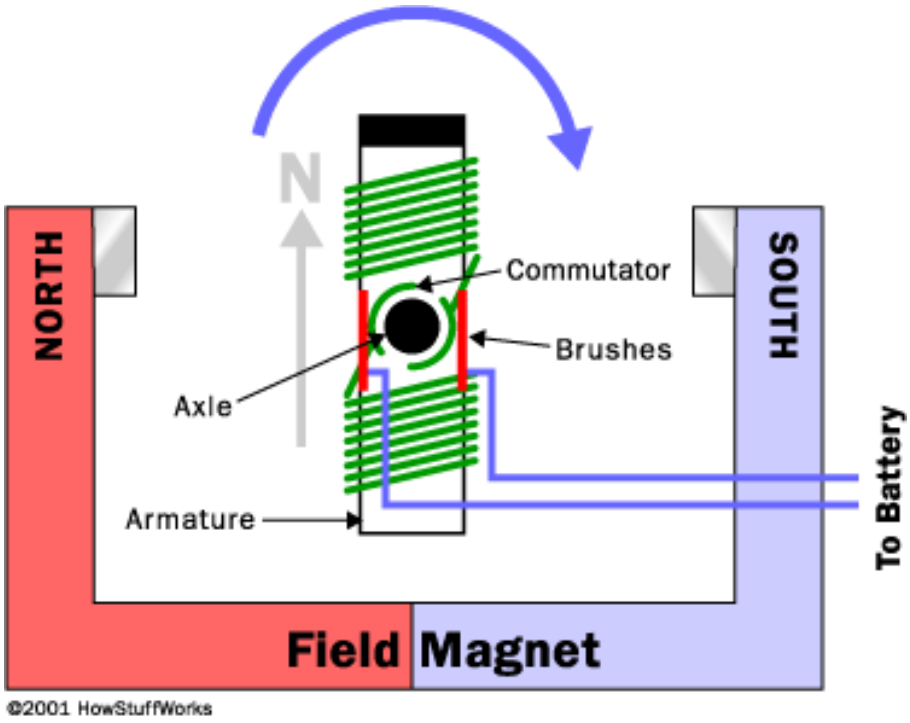

Figure 1: General Principle of Electric Motors
(taken from HowStuffWorks.com)

2.2.4 Torque Production

After the rotor starts turning, the shaft will have torque. Different types of motors have different methods of torque production. For example, in an induction motor, slip creates the torque. Slip occurs since the moving magnetic field in the stator is always faster than the speed of the rotor.

2.2.5 Speed Production

As the rotor shaft is turning, it will have some speed. Again, in an induction motor, speed can be adjusted by changing the input power frequency. Also, during the design, based on the requirements, the number of poles can be decided. A greater number of poles would provide a higher speed.

2.3 Electric Motor Types

Based on the operating principle, motors can be divided into three groups: magnetic, electrostatic, and piezoelectric. Electric motors can also be AC or DC driven. In general, based on motion type, electric motors can be rotating, linear, or spherical.

2.4 Conclusion

The literature survey provides clarity in understanding the current stage of the problem. In a spherical electric motor, there are several challenges, such as actuation, bearing, and position control. The previous brief information about electric motors and types is helpful and makes the investigation for different types of electric motors more efficient. In Chapter 3, a new type of electric motor, the spherical electric motor will be introduced.

CHAPTER 3

WORKING PRINCIPLES AND STRUCTURE OF SEM

3.1 Introduction

The spherical electric motor differs from other types of motors mainly in its motion style. In today's world, when the word "motor" is heard, people usually think of a rotating device, when in fact, there are both linear and spherical motors. Linear motors are used in different applications, as discussed previously. However, spherical motors are not yet in use. Once an SEM is in use, it might replace some rotating and linear motors more efficiently.

Figures 2 and 3 show an SEM in detail. The output shaft of an SEM moves with three DOF, whereas the output shafts of rotating and linear motors move with one degree of freedom. Naturally, the actuation method of an SEM becomes quite different from rotating and linear motors. SEMs designed to date have different methods for actuation, as discussed earlier.

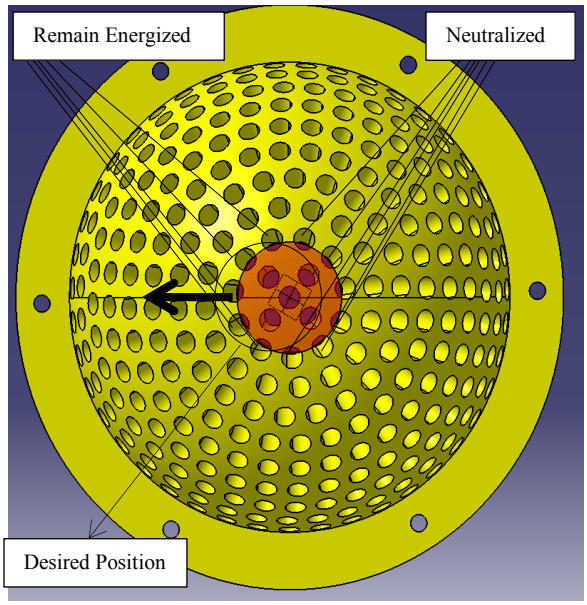

Figure 2: Bottom Part of SEM Stator in Detail

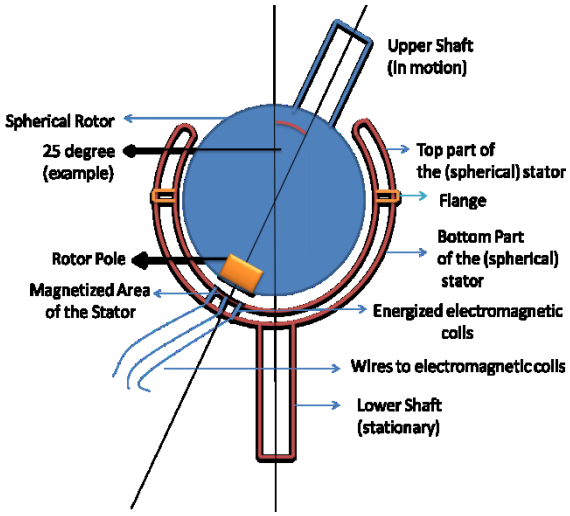

Figure 3: Low-Speed 2-DOF Joint SEM

In this chapter, first, a new methodology for SEM actuation will be discussed. Then, based on the methodology, the structure of the SEM will be presented.

3.2 Methodology

Multi-DOF actuation is attained by a "moving magnetic field" in the stator.

Moving Magnetic Field

As shown previously, Figure 2 illustrates the bottom part of an SEM stator. Electromagnetic coils (not shown) are located in the circular housings all around the stator. The diameter of the each housing is 5 mm. A circular group of housings with coils inside create the magnetic field. During operation, an estimated diameter of the magnetic field is 30 mm. In Figures 2 and 3, the orange areas represent the rotor pole. Figure 4 shows the low-speed 3-DOF SEM joint, and Figure 5 shows the interaction of the pole and magnetic field (red circular area consists of individual electromagnetic coils).

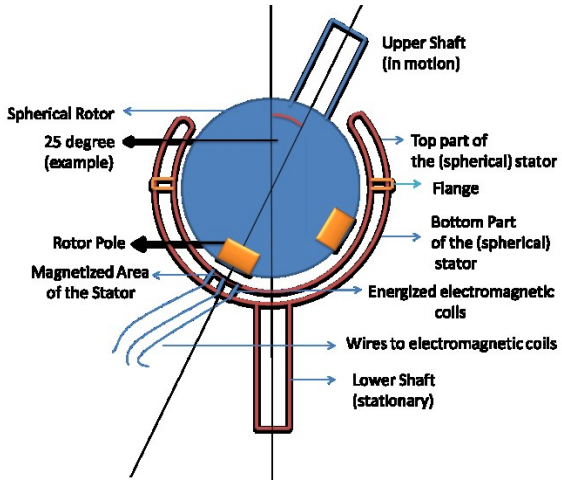

Figure 4: Low-Speed 3-DOF Joint SEM

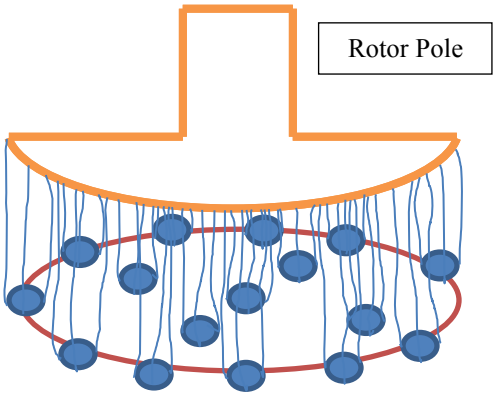

Moving Magnetic Field Created by Individual Coils

Figure 5: Interaction of Pole and Magnetic Field

Moving the magnetic field is achieved by energizing and neutralizing the related individual coils. To move the magnetic field in the direction of the arrow, the coils need to be energized and neutralized, as shown previously in Figure 2. In fact, liquid crystal display (LCD) methodology is similar to this method in terms of motion effect [51]. The method used by Shan

et al. [48] for magnetic suspension is similar to the method here in terms of force effect. Because the goal is to move the magnetic field with proper resolution and force effect, each individual coil needs to be controlled.

Rotor

Located inside the stator, the rotor has a number of poles based on the structure of the SEM. However, the common pole, which all structures have, is located on the axis of the upper shaft but on the opposite side of the rotor. The pole is embedded in the rotor, and its surface is even with the rotor surface. The poles are embedded with a ball bearing in the rotor of the 3-DOF SEM, as shown in Figure 6. The diameter of each pole is 30 mm. The gap between the rotor and the stator is 0.5 mm. The rotor is supported by eight transfer bearings (not shown). Structural details will be provided in the next section.

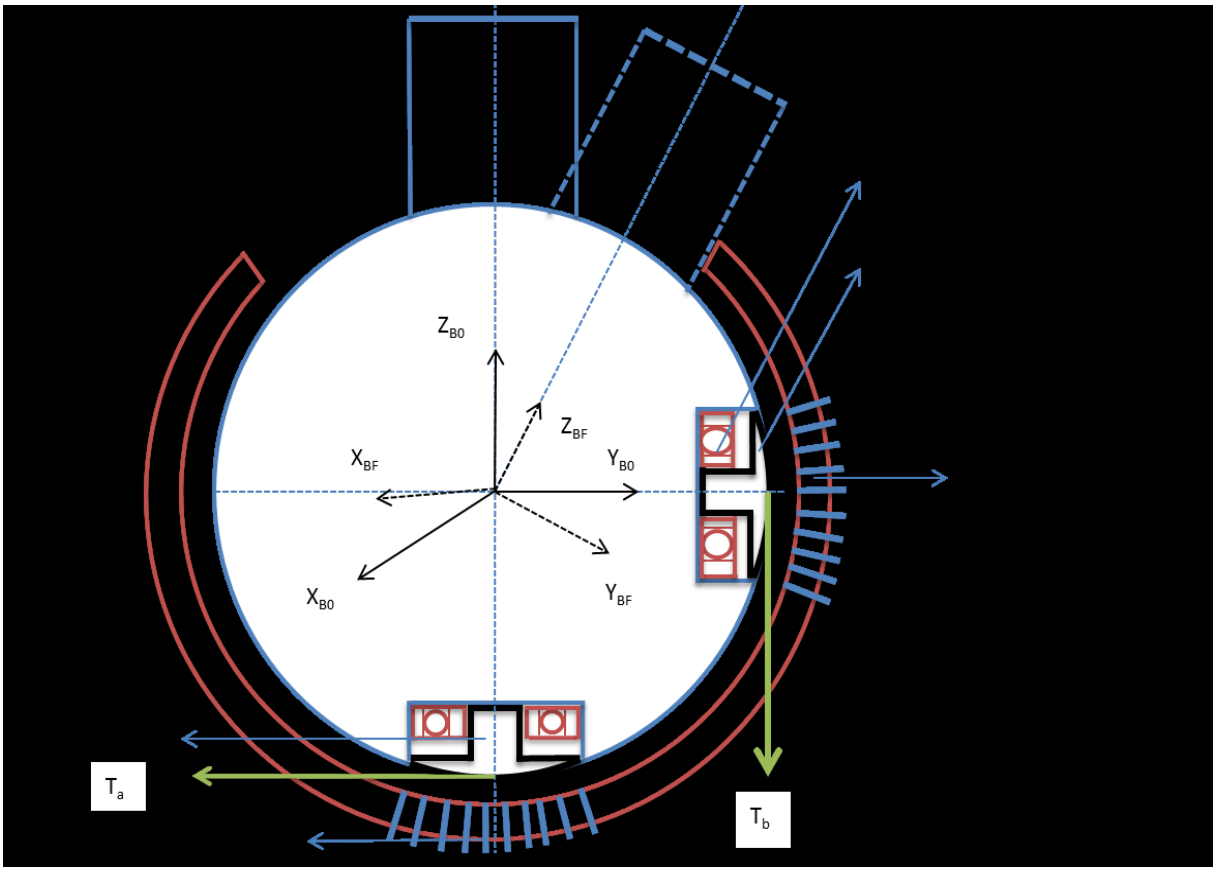

Figure 6: Low-Speed 3-DOF Joint SEM with Rotor and Stator Poles

Motion of Rotor

In the 3-DOF SEM, both the moving magnetic fields in the stator are coupled with the rotor poles. Figure 6 shows the coupling of both magnetic fields with corresponding rotor poles. For a given desired trajectory of rotor shaft, the trajectories of magnetic fields can be calculated.

3.3 Structure of SEM

SEM has a different structure than conventional rotary motors due to the multi-DOF motion. Based on speed, torque, and motion-DOF requirements, an SEM can be structured in three different ways: low-speed 2-DOF joint SEM, low-speed 3-DOF joint SEM, and high-speed 3-DOF wheel and propeller SEM. Technical structures and working principles of all three actuators will be presented. However, the low-speed 3-DOF joint SEM will be studied in detail in this research.

Low-Speed 2-DOF Joint SEM

In applications in which pitch and yaw DOF are needed, a low-speed 2-DOF joint SEM can be used. In this case, as shown in Figures 2 and 3, the orange part represents the rotor pole, which is on the axes of the upper shaft. This configuration provides 2-DOF by moving the magnetic field. By energizing and neutralizing individual coils, the magnetic field moves around the stator.

Low-Speed 3-DOF Joint SEM

If roll, pitch, and yaw motions are needed together, then adding another pole 90 degrees from the previous pole is sufficient. However, this time, both poles need to rotate to prevent motion singularity. By using ball bearings, as shown previously in Figure 6, both poles can be free to rotate. Therefore, 3-DOF can be attained simultaneously with no motion singularity. In the stator, two moving magnetic fields would be observed. They are 90 degrees apart from each

other by using the center of the stator as a reference. Figure 4 shows a 3-DOF joint SEM (moving magnetic field for the second pole is not shown). As in the previous case, the moving magnetic fields on the stator are coupled with rotor poles, and the rotor moves with 3-DOF.

High-Speed 3-DOF Wheel and Propeller SEM

When it is necessary to have 3-DOF motion in high speed, an efficient structure can be designed. The type of actuation in the previous two cases has some speed-level limitations. The common pole in all structures is still providing pitch and yaw motions, but for the high-speed roll motion, the rotor must have four additional poles 90 degrees apart from each other on its equator. All five poles are free to rotate by using ball bearings to prevent motion singularity. Figure 7 shows a high-speed 3-DOF wheel and propeller SEM.

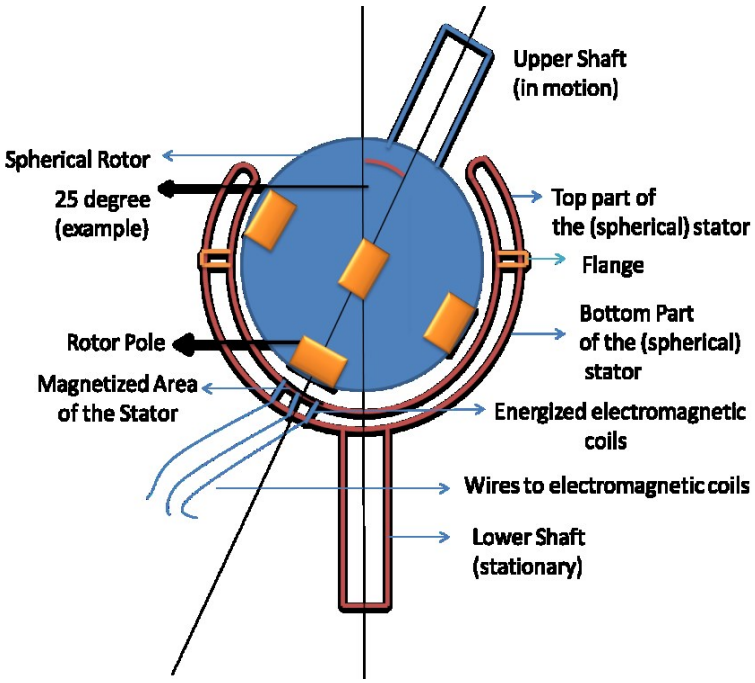

Figure 7: High-Speed 3-DOF Wheel and Propeller SEM

The rotor pole in the back is not visible. The moving magnetic field is shown for only a common pole. The rotor poles on the equator interact with their corresponding moving magnetic fields on the stator. However, the interaction between equator poles and moving magnetic fields

on the stator is different than in the previous cases. The interaction in this case is repulsion and attraction as in a conventional stepper motor. It is possible to generate different directions of magnetic force in moving magnetic fields (moving stator pole).

3.4 Conclusion

As shown, the working principles of an SEM are quite different than for conventional motors. Based on the requirements, different SEMs can be built. A high-speed SEM uses the same method as conventional stepper motors. However, stator arrangement is completely different in an SEM.

CHAPTER 4

MAGNETIC FIELD AND TORQUE MODELING OF SEM

4.1 Introduction

Magnetic field modeling is an essential step for torque modeling. The actuation method described in Chapter 3 mainly depends on the moving magnetic fields on the stator. In this chapter, the methodology to generate moving magnetic fields in the stator and resultant torques affecting the rotor for a low-speed 3-DOF joint SEM will be presented.

4.2 Methodology

In the stator, the moving magnetic field is generated by individual coils. As shown previously in Figure 5, the group of coils forms a circular area that coincides with the rotor pole. Blue circles represent the tip of an electromagnetic core around which a wire coil is installed. The complete electromagnetic illustration of an individual core with coil and rotor pole is shown in Figure 8.

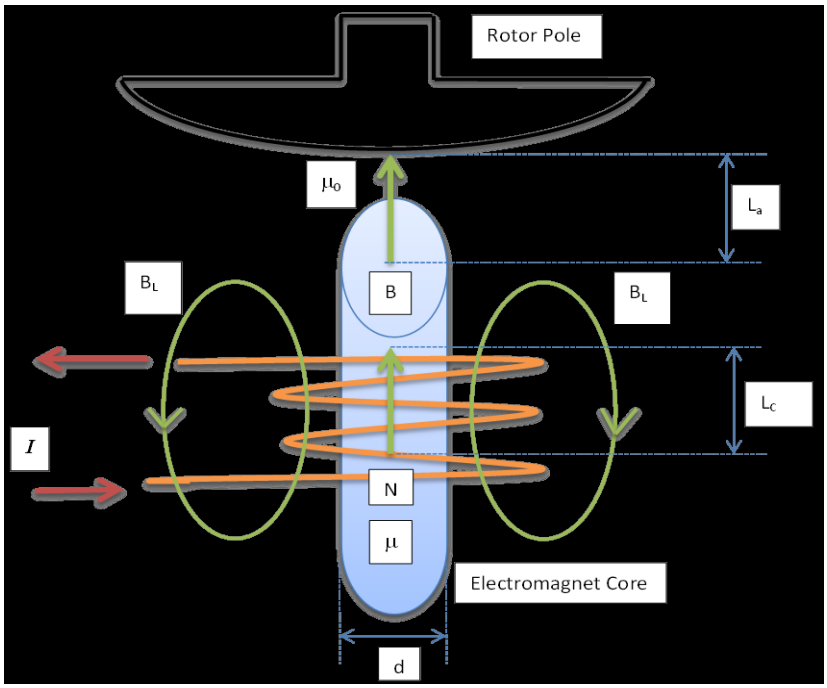

Figure 8: Single Electromagnetic Coil and Rotor Pole

Magnetic Field

Assuming that eddy currents are ignored, when electrical energy W is applied to the coil, it is converted to magnetic field energy. Therefore,

$$W = \int_0^t vI\, dt \tag{1}$$

where I is the applied current, and v is the voltage during time t.

By Faraday's Law, voltage v is defined by

$$v = N\frac{d\Phi}{dt} \tag{2}$$

where N is the number of turns in the coil, and Φ is the magnetic flux. Replacing v in equation (1) with v in equation (2) yields

$$W = \int_0^{\Phi} NI d\Phi \tag{3}$$

Magnetic flux is produced by a magneto motive force (MMF), F_m, which is calculated by Ampere's Law:

$$F_m = NI \tag{4}$$

The intensity of the magnetic field is called magnetic field strength, H, and it is given by

$$H = \frac{F_m}{L_c} \tag{5}$$

where L_C is the length of the magnetic field in the electromagnetic core. Therefore, $NI = HL_c$ and

$$W = \int_0^{\Phi} HL_c d\Phi \tag{6}$$

Flux density, B, is calculated by dividing flux, Φ by the cross-sectional area of the core, A; therefore,

$$B = \frac{\Phi}{A} \Rightarrow d\Phi = A\, dB \tag{7}$$

Substituting equation (7) into equation (6) results in $W = \int_0^B HL_cA\, dB$, the magnetic field energy in the core. To find the intensity of the energy W_i, W is divided by the volume of the core:

$$W_i = \frac{\int_0^B HL_cA\, dB}{L_cA} \Rightarrow W_i = \int_0^B H\, dB \tag{8}$$

As can be seen, W_i has H and B terms, which are evaluated in terms of magnetization curves. In real-life applications, magnetization curves are not straight, but they are assumed to be straight here. Figure 9 shows the gradient of the magnetization curve, which gives μ permeability of the core.

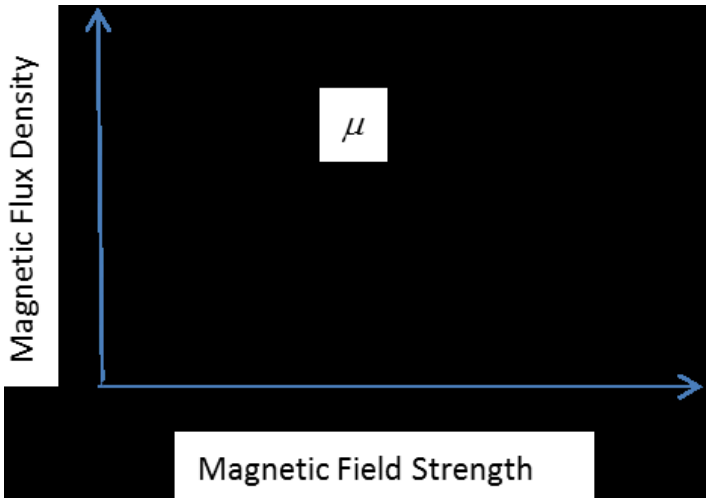

Figure 9: Magnetization Curve (assumed to be straight)

Therefore,

$$\mu = B/H \tag{9}$$

Finally,

$$W_i = \int_0^B \frac{B}{\mu}\, dB \Rightarrow W_i = \frac{B^2}{2\mu} \tag{10}$$

As shown, the product of the number of turns in the coil N and the current on the wire I yields NI, which is the ampere turns. The magnetic field is proportional to NI. The closed-loop magnetic fields B_L do not have any effect on the exerted force by the magnetic field. As shown

previously in Figure 8, L_a is the length of the magnetic field in the space between the electromagnetic core and the rotor pole, and μ_o is the permeability of the space between the electromagnetic core and the rotor pole.

4.3 Magnetic Field and Exerted Force

When current flows through the coil, a magnetic field, as shown previously in Figure 8, and magnetic force result. Assuming the magnetic field is uniform in the gap, W_i is multiplied by the gap volume to obtain the magnetic field energy W:

$$W = \frac{B^2}{2\mu} L_a A \tag{11}$$

Now, the energy change within the gap between the core and the rotor pole provides the force on the rotor applied by the electromagnetic coil as

$$F = \frac{dW}{dL_a} \tag{12}$$

Therefore,

$$F = \frac{B^2 A}{2\mu_0} \tag{13}$$

Equations $H = \frac{F_m}{L_c}$ and $\mu = B/H$ are used for the core, but they can also be used for the gap in the above assumptions. Therefore,

$$B = \frac{F_m \mu_0}{L_a} \tag{14}$$

The force will be

$$F = \frac{\left(\frac{F_m \mu_0}{L_a}\right)^2 A}{2\mu_0} \tag{15}$$

Canceling the same multipliers results in the following force equation:

$$F = \frac{F_m^2 \, \mu_0 \, A}{2L_a^2} \tag{16}$$

Since it is known that $F_m = NI$, the force applied by the electromagnetic coil can be rewritten as

$$F = \frac{N^2 I^2 \mu_0 A}{2L_a^2} \tag{17}$$

It is assumed that the diameter of the electromagnetic core is very small compared to the rotor pole, so the interaction between individual coils can be ignored. Therefore, the resultant torque T is given by

$$T = \sum_{i=1}^{n} F_i \, r \tag{18}$$

where n is the number of coils within a moving magnetic field in the stator, and r is the radius of the rotor assembly. Since there are two poles in the rotor, T_a and T_b torques are applied to the rotor, as shown previously in Figure 6, to yield

$$T_a = \sum_{i=1}^{n_a} r \frac{N^2 I_{a_i}^2 \mu_0 A}{2L_a^2} \tag{19}$$

where n_a is the number of electromagnetic coils, and I_a is the current amount applied to an individual coil within the moving magnetic field, thus creating T_a. Similarly,

$$T_b = \sum_{i=1}^{n_b} r \frac{N^2 I_{b_i}^2 \mu_0 A}{2L_a^2} \tag{20}$$

where n_b is the number of electromagnetic coils, and I_b is the current amount applied to an individual coil within the moving magnetic field, thus creating T_b.

Now, the important question is how individual coils will be energized in each moving magnetic field. As shown previously in Figure 2, the large orange piece represents the rotor pole and the small red circles represent the energized coils. To move the moving magnetic field to the desired position, the coils that are in the same direction as the arrow will remain energized, and the coils that are on the opposite side of the arrow will be neutralized. Also, if needed, more coils in the arrow direction will be energized. Below, systematic steps are given for the moving

magnetic fields on the stator. Torques T_a and T_b cause the rotor to move in 3-DOF. The torques created at one time by the coils within two magnetic fields is computed above. Since the magnetic fields are moving, any coil around the stator is a candidate to be energized. There are two poles to be moved, so two inputs are needed—u_a and u_b—the sizes of which are (n × 1), where n is the number of coils within the stator.

Special Case of Low-Speed 3-DOF Joint SEM Moving Magnetic Field Procedure

To describe the stator poles (moving magnetic fields) simply, it is assumed that the rotor pole, which is on the equator of the rotor, remains stationary (it is coupled with the stator pole and remains in the same position), i.e., the SEM will be moving in 2-DOF by the "south rotor pole" and its stator pole. Figure 10 shows the south stator pole and its energizing and neutralizing certain coils. It is assumed that coupling is perfect between the stator pole and the rotor pole during the low-speed motion.

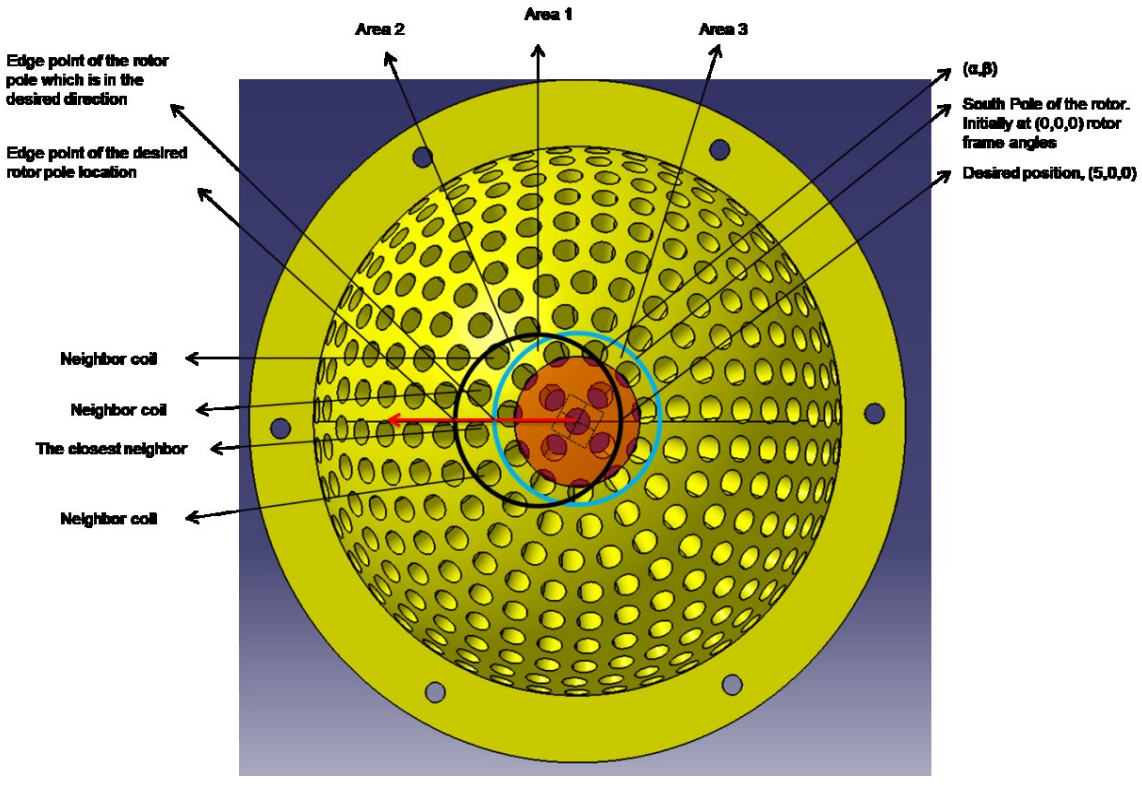

Figure 10: Bottom Part of Spherical Stator and Its South Pole Motion
(lower shaft is uninstalled)

Steps for South Pole of Stator

Step 1:

Set the rotor at the initial conditions, which is zero for all angles. Then, based on initial conditions and known mapping of stator coils by their spherical coordinates, the coils energized are already identified. Each coil can be located as follows:

$$S_i = \begin{bmatrix} cos\alpha cos\beta \\ cos\alpha sin\beta \\ sin\alpha \end{bmatrix}$$

where α indicates latitude, and β indicates longitude.

Step 2:

Obtain the desired trajectory, which, for simplicity, is assumed as follows:

$$\boldsymbol{\theta_d} = \begin{bmatrix} \phi \\ \theta \\ \psi \end{bmatrix} = \begin{bmatrix} 0.1 \\ 0 \\ 0 \end{bmatrix}$$

The desired trajectory is three dimensional; however, only ϕ will be changed. Based on the desired trajectory and current location of the rotor pole, the edge point of the rotor pole, which is located on the axis of desired trajectory, is identified. Therefore, the desired edge point, current edge point, and center of rotor will be on the same axis as shown previously in Figure 10.

Step 3:

Search the array of stator coils, and identify the neighbor coils of the current edge point. Select the closest neighbor coil and its neighbors within Area 2 to be energized. Select the coils within Area 3 to be neutralized. Finally, select the coils within Area 1 to be left energized.

The above three steps of the algorithm are repeated when the current edge point of the rotor reaches the edge point of the desired rotor location. Thus far, a complex stator pole motion has been covered. It is worth saying that motion accuracy is guaranteed by the interaction between each coil and the rotor pole. The interaction for other coils is shown in Figure 11.

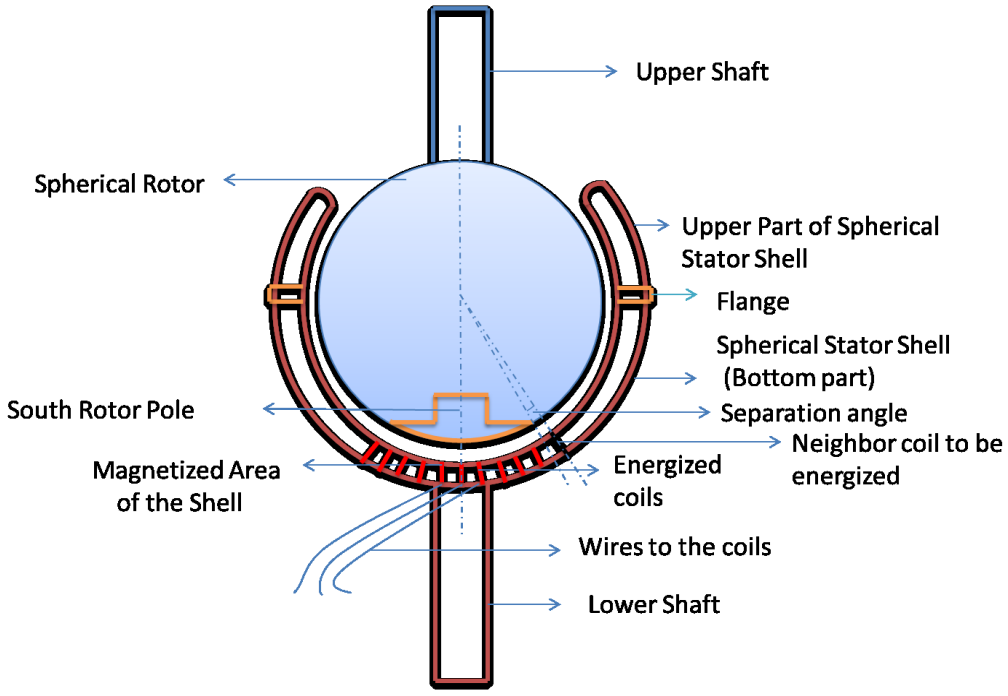

Figure 11: Energized Stator Coils, Rotor Pole, and Neighbor Coil with Separation Angle

Since the coordinates of each coil and rotor pole are known, the final position vector s_i of the stator coils in the rotor frame can be calculated by using a rotation matrix, which will be introduced in Chapter 5. Since the interaction between the stator coils and the rotor pole is calculated by utilizing the direction vector, as shown later in equation (24), multiple coils will be energized accordingly to satisfy the desired torque input component in each dimension. The desired torque input components will be calculated in Chapter 6.

The above three-step algorithm can be extended for the pole at the equator as well. It is straightforward to calculate the desired motion of the pole based on the given trajectories. In previous equations (19) and (20), the torque values are at the initial time when the rotor is stationary. During the motion, different coils will be energized and neutralized. There will be a separation angle δ for each individual coil. Figure 11 shows the SEM coils and rotor pole with the separation angle, which is between the axis of the rotor-pole edge and the axis of the nearest coil. The torque value is also dependent on the separation angle. In other words, the torque

function *f(δ)* needs to be included in the torque equation. The torque function can be calculated either by an experiment or by finite element analysis method. However, Figure 12 gives conceptual information about the separation angle and torque function [38].

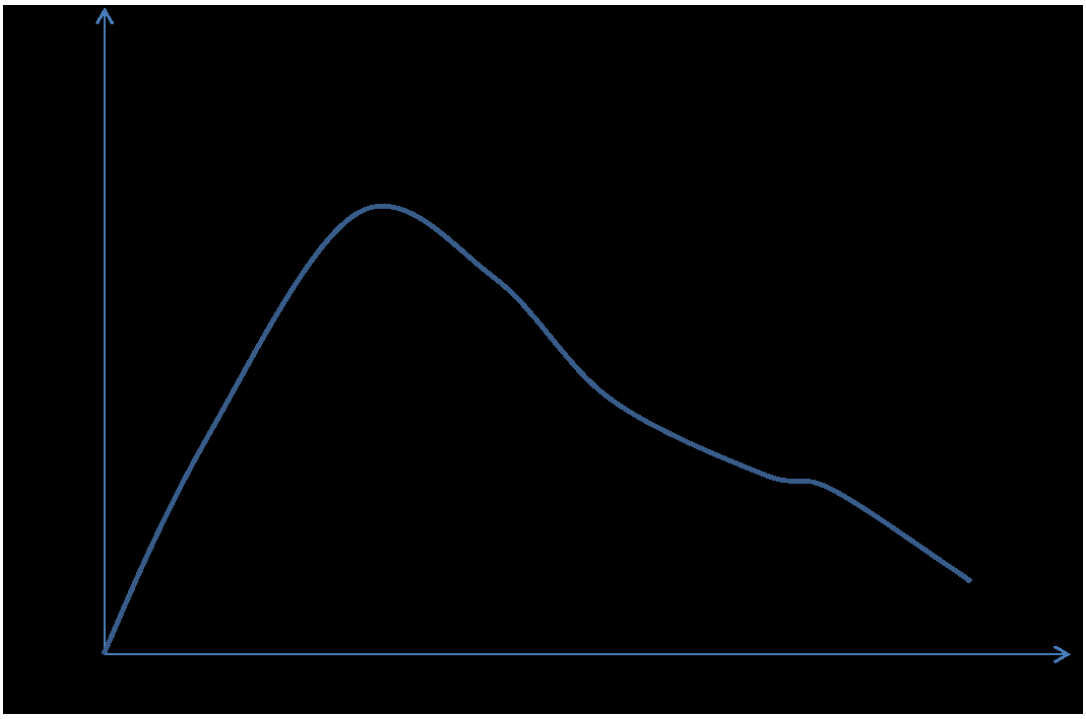

Figure 12: Expected Relationship *f(δ)* between Separation Angle and Torque

Also, the direction of torque *d* must be included in the torque equation since the desired input torque components will be calculated using the computed torque model, as explained in Chapter 5. In the previous equations (19) and (20), except for the applied current, the remaining terms are constants. With inclusion of the torque function and direction, equations (19) and (20) can be rewritten as

$$T_a = GI_{a_i}^2 \tag{21}$$

$$T_b = GI_{b_i}^2 \tag{22}$$

where *G* is the torque matrix and includes function and direction of the torque. Therefore, *G* can be written as

$$G = f(\delta) \bullet d \tag{23}$$

where

$$d = \frac{r \times s_i}{\|r \times s_i\|} \tag{24}$$

In equation (24), r is the coordinates of the edge of the rotor pole, and s_i is the coordinates of a stator coil.

Thus far, for clarification, two different regions in the stator have been studied separately. However it is possible to have one torque equation based on equations (21), (22), and (23), as follows:

$$T = GI_i^2 \tag{25}$$

where G is the torque matrix and includes torque function and torque direction of each individual coil in the stator. Therefore,

$$G = [\, f_1(\delta_1) \bullet d_1 \qquad f_2(\delta_2) \bullet d_2 \ldots\ldots\ldots f_n(\delta_n) \bullet d_n \,] \tag{26}$$

where n is the number of stator coils. Although there are two rotor poles, they interact with different individual coils. In equation (26), the term $g_i = f_i(\delta_i) \bullet d_i$ has a matrix size of 3 x 1 since the direction of the torque has components in three axes. Therefore, total torque can be computed as

$$T = \begin{bmatrix} T_x \\ T_y \\ T_z \end{bmatrix} = GI^2 = [\, g_1 \;\; g_2 \ldots\ldots\ldots\; g_n] \begin{bmatrix} I_1^2 \\ I_2^2 \\ \vdots \\ I_n^2 \end{bmatrix} \tag{27}$$

Inverse Torque Model

In order to find the required current to apply to the SEM, an inverse torque model is needed. The required torque will be calculated in Chapter 5 by using the computed torque model. Therefore, torque and torque matrix are calculated and the current can be derived as follows:

$$\begin{bmatrix} I_1^2 \\ I_2^2 \\ \vdots \\ I_n^2 \end{bmatrix} = G^{-1}T \text{ , n=3} \tag{28}$$

$$\begin{bmatrix} I_1^2 \\ I_2^2 \\ \vdots \\ I_n^2 \end{bmatrix} = (G^T G)^{-1} G^T T \text{ , n=1, 2} \tag{29}$$

$$\begin{bmatrix} I_1^2 \\ I_2^2 \\ \vdots \\ I_n^2 \end{bmatrix} = G^T (GG^T)^{-1} T, n = 3,4, \dots \dots \dots n \tag{30}$$

The left inverse of the torque matrix in equation (29) and the right inverse of the torque matrix in equation (30) are used to prevent singularities. For the experiments, equations (28) and (29) may be used. Under normal conditions, equation (30) is the main inverse torque model to apply.

4.4 Conclusion

In the described SEM, the stator structure is the major part. It includes a number of coils distributed uniformly around it. This circular group of coils creates the moving magnetic field, which resembles the methodology in a magnetic suspension system and also a liquid crystal display system. The moving magnetic fields are coupled with rotor poles as they are moving, and the SEM realizes the three-dimensional motion. In torque modeling, angular distances between the coils and rotor poles, and torque functions are the main parameters. Torque functions can be calculated by experiments or utilizing finite element analysis. Angular distances between the coils and rotor poles are calculated by using rotor pole positions and coil positions. The inverse torque model provides the current values for each coil.

CHAPTER 5

DYNAMIC MODELING OF SEM

5.1 Introduction

In this chapter, the methodology for dynamic modeling using Lagrange's equation will be presented, and a mathematical dynamic model will be derived for the system shown previously in Figure 12.

5.2 Methodology

In a SEM with 2-DOF, deriving the equations of motion is straightforward. First, using the Jacobian matrix, the coordinates of the rotor are defined in order to obtain the velocities. Second, using a Lagrange model of the system, relations between rotation angles and velocities can be determined.

However, in an SEM with 3-DOF, defining the coordinates is not the same as in an SEM with 2-DOF. Instead, two different axes are considered: body axes and reference axes. Then, the body orientation can be defined by defining the angles between the body axes and the reference axes. These angles are called Euler angles. At initial conditions, body and reference axes may or may not align, but for simplicity, it is assumed that they are aligned at initial conditions. As shown previously in Figure 6, X_{B0}, Y_{B0}, and Z_{B0} are the body axes of the rotor at the initial time. The SEM shaft drawn with dashed lines is in its final position. The rotor is rotated first (ψ degrees) about the Z-axis, second (θ degrees) about the new Y-axis, and finally (ϕ degrees) about the most recent X-axis. Also in Figure 6, the final condition of the body axes, X_{BF}, Y_{BF}, and Z_{BF}, are drawn with dashed lines.

Friedland [53] describes the rotation matrix $T_{BR,}$ which rotates the X_{B0}, Y_{B0}, and Z_{B0} body axes to the final condition body axes, X_{BF}, Y_{BF}, and Z_{BF}, as follows:

$$T_{BR} = \begin{bmatrix} cos\theta cos\psi & -cos\theta sin\psi & sin\theta \\ cos\psi sin\phi sin\theta + cos\phi sin\psi & cos\phi cos\psi - sin\phi sin\theta sin\psi & -cos\theta sin\phi \\ -cos\phi cos\psi sin\theta + sin\phi sin\psi & cos\psi sin\phi + cos\phi sin\theta sin\psi & cos\phi cos\theta \end{bmatrix} \quad (31)$$

The term T_{BR} is an orthogonal matrix, so $(T_{BR})^{-1} = (T_{BR})^{T} = T_{RB}$, where T_{RB} is the matrix that rotates the body axes back to their initial condition. The term T_{BR} is the product of three rotation matrices in the order of rotation about the *Z*, *Y*, and *X* axes. Each multiplier represents the rotation about an axis.

For this SEM, dynamical modeling was done by Lagrange's equation:

$$\frac{d}{dt}\left(\frac{\partial L}{\partial \dot{\theta}}\right) - \frac{\partial L}{\partial \theta} = T \quad (32)$$

where *L* is the Lagrange multiplier, representing both kinetic and potential energy. Since the system consists of a rigid rotor inside a stationary stator, potential energy does not exist. Kinetic energy is generated by the motion of the rotor. The angle for each degree of freedom is θ, and the torque for each degree of freedom is *T*. The rotor is moving with 3-DOF, so there are three equations.

Energy

In the SEM, naturally, potential energy does not exist. The only countable energy in SEM dynamics is kinetic energy, as follows:

$$L = \frac{1}{2}J_x\omega_x^2 + \frac{1}{2}J_y\omega_y^2 + \frac{1}{2}J_z\omega_z^2 \quad (33)$$

where *J* is the moment of inertia, and for simplicity, $J_x = J_y = J_z = 1$ is assumed. From the work of Guo and Xia [43] and Friedland [53], the components of angular velocities can be written as ω_x, ω_y, and ω_z, which are the projected angular velocities onto the rotating body axes. In the stator frame by using Euler angles, components of the angular velocities are described as

$$\begin{bmatrix} \omega_x \\ \omega_y \\ \omega_z \end{bmatrix} = \begin{bmatrix} cos\theta cos\psi & sin\psi & 0 \\ -cos\theta sin\psi & cos\psi & 0 \\ sin\theta & 0 & 1 \end{bmatrix} \begin{bmatrix} \dot{\phi} \\ \dot{\theta} \\ \dot{\psi} \end{bmatrix} \quad (34)$$

5.3 Dynamic Model

By utilizing the Lagrange equation, the system is simplified for modeling. In fact, the nature of an SEM assists in a simplified dynamical model since all degrees of freedoms originate from the same common center point, which is the center of the rotor ball. Substituting equations (33) and (34) into equation (32), the dynamic model of SEM can be found as follows:

$$\ddot{\phi} + \ddot{\psi}\sin\theta + \dot{\theta}\,\dot{\psi}\cos\theta = T_x \tag{35}$$

$$\ddot{\theta} - \dot{\phi}\,\dot{\psi}\cos\theta = T_y \tag{36}$$

$$\ddot{\psi} + \ddot{\phi}\sin\theta + \dot{\phi}\,\dot{\theta}\cos\theta = T_z \tag{37}$$

In equations (35), (36), and (37), it is worth mentioning that the inertia terms are typed in red, and the Coriolis centripetal terms are typed in blue. They can be restructured by using the general dynamic matrix form:

$$\boldsymbol{M}(\boldsymbol{\theta})\,\ddot{\boldsymbol{\theta}} + \boldsymbol{C}\left(\boldsymbol{\theta}, \dot{\boldsymbol{\theta}}\right)\dot{\boldsymbol{\theta}} = \boldsymbol{T} \tag{38}$$

where $\boldsymbol{M}(\boldsymbol{\theta})$ is the inertia matrix, and $\boldsymbol{C}\left(\boldsymbol{\theta}, \dot{\boldsymbol{\theta}}\right)$ is the Coriolis and centripetal matrix:

$$\boldsymbol{M}(\boldsymbol{\theta}) = \begin{bmatrix} 1 & 0 & \sin\theta \\ 0 & 1 & 0 \\ \sin\theta & 0 & 1 \end{bmatrix} \quad ; \quad \boldsymbol{C}\left(\boldsymbol{\theta}, \dot{\boldsymbol{\theta}}\right) = \begin{bmatrix} 0 & \dot{\psi}\cos\theta & 0 \\ -\dot{\psi}\cos\theta & 0 & 0 \\ \dot{\theta}\cos\theta & 0 & 0 \end{bmatrix}$$

where $\boldsymbol{T}$ is the torque control input matrix, and $\boldsymbol{\theta}$ is the Euler angles (ϕ, θ, ψ) for the SEM. The first and second derivations of Euler angles provide angular speeds and angular accelerations, respectively.

5.4 Conclusion

The Lagrange equation provides a clear perspective of the dynamics of the SEM. The inertia and Coriolis terms can be simply decoupled to reconstruct the matrix form of the dynamic system. This decoupling is expected to be helpful for an efficient control algorithm in Chapter 6.

CHAPTER 6

CLOSED-LOOP CONTROLLER FOR SEM

6.1 Introduction

Control of an SEM is similar to other single-degree-of-freedom motors after certain steps are taken [40]. In this research, a control approach is based on a dynamic decoupling computed torque model (DDCTM). The decoupling procedure becomes more efficient in an SEM that has all degrees of freedoms originating from the same common center point. Nonlinear couplings in each axis can be considered as disturbance torque [43].

For simplicity, control torque, load torque, and disturbance torque will be considered under one notation $\boldsymbol{T} = [T_x, T_y, T_z]$, where $\boldsymbol{T}$ is the control torque under assumptions of no load and no disturbance in the system.

6.2 Methodology

In an SEM, motion is about the center single point. Therefore, highly nonlinear couplings are observed in the equation of motion described in equations (35), (36), and (37). Nonlinear inter-axis couplings, typed in red and blue, may be considered as disturbance torques. Therefore, equations (35), (36), and (37) can be modified as follows

$$\ddot{\phi} = T_x \tag{39}$$

$$\ddot{\theta} = T_y \tag{40}$$

$$\ddot{\psi} = T_z \tag{41}$$

In equations (39), (40), and (41), the moment of inertia is 1 and no-disturbance and no-load assumptions are made. Thus, each degree of freedom motion can be separately controlled by utilizing decoupling. Therefore, the control law is introduced as [43, 50, and 52]

$$\boldsymbol{M}(\boldsymbol{\theta})\,\boldsymbol{u} + \boldsymbol{C}\left(\boldsymbol{\theta}, \dot{\boldsymbol{\theta}}\right)\dot{\boldsymbol{\theta}} = \boldsymbol{T} \tag{42}$$

where u is the new control input [52]; therefore,

$$\ddot{\theta} = \boldsymbol{u} \tag{43}$$

Trajectory Tracking

For continuous accuracy of the position, desired trajectories $\boldsymbol{\theta_d}$ are used so that dynamic tunings can be performed. Consequently, $\dot{\boldsymbol{\theta}}_{\boldsymbol{d}}$ is the desired angular velocity vector, and $\ddot{\boldsymbol{\theta}}_{\boldsymbol{d}}$ is the desired angular acceleration vector. The continuous derivation of $\boldsymbol{\theta_d}$ is assumed, so a continuous trajectory exists.

The difference between the desired and actual angles is called *error* and is represented as

$$\boldsymbol{e} = \boldsymbol{\theta}_d - \boldsymbol{\theta} \tag{44}$$

Error changes as the SEM moves. The changing rate of error can be stated as

$$\dot{\boldsymbol{e}} = \dot{\boldsymbol{\theta}}_d - \dot{\boldsymbol{\theta}} \tag{45}$$

In the next section, a controller will be designed with the goal that error becomes zero. Therefore, the actual and desired trajectories match.

6.3 Design

The DDCTM algorithm guaranties exponentially stable closed-loop dynamics. Each degree of freedom is controlled separately. Error is controlled to be zero dynamically. Using equations (43), (44), and (45), the goal for error is as follows [43]:

$$\left(\ddot{\boldsymbol{\theta}}_{\boldsymbol{d}} - \ddot{\boldsymbol{\theta}}\right) + \boldsymbol{K_d}\left(\dot{\boldsymbol{\theta}}_d - \dot{\boldsymbol{\theta}}\right) + \boldsymbol{K_p}(\boldsymbol{\theta}_d - \boldsymbol{\theta}) = \mathbf{0} \tag{46}$$

where $\boldsymbol{K_d}$ is a positive definite derivative controller, and $\boldsymbol{K_p}$ is a positive definite proportional controller. Both are 3 x 3 diagonal matrices. From equation (46), error equation can be obtained as

$$\ddot{\boldsymbol{e}} + \boldsymbol{K_d}\dot{\boldsymbol{e}} + \boldsymbol{K_p}\boldsymbol{e} = \mathbf{0} \tag{47}$$

Substituting equations (46) and (43) into equation (42), yields the following general control law for SEM:

$$\boldsymbol{T} = \boldsymbol{C}\left(\boldsymbol{\theta}, \dot{\boldsymbol{\theta}}\right)\dot{\boldsymbol{\theta}} + \boldsymbol{M}(\boldsymbol{\theta})(\ddot{\boldsymbol{\theta}}_{\boldsymbol{d}} + \boldsymbol{K_d}\dot{\boldsymbol{e}} + \boldsymbol{K_p}\boldsymbol{e}) \tag{48}$$

From equation (47), it can be stated that the error and the error changing rate will be driven to zero, and trajectory tracking will be guaranteed. As a result, a globally asymptotically stable system is also promised.

6.4 Simulation

The DDCTM algorithm in equation (48) is an efficient algorithm for an SEM for several reasons. Dynamic decoupling allows each degree of freedom to be controlled separately. For different initial conditions, performance of the system is still high. Also, error handling guarantees the stability.

Simulation with Zero Initial Conditions

All initial position angles are set to zero, and the desired trajectory is set as

$$\boldsymbol{\theta_d} = \begin{bmatrix} \sin(2t) \\ \cos(1.7t) \\ \sin(2.5t) \end{bmatrix} \tag{49}$$

The derivative and proportional controllers are set as diagonal matrices:

$$\boldsymbol{K_d} = \begin{bmatrix} 6 & 0 & 0 \\ 0 & 10 & 0 \\ 0 & 0 & 7 \end{bmatrix} \tag{50}$$

$$\boldsymbol{K_p} = \begin{bmatrix} 10 & 0 & 0 \\ 0 & 20 & 0 \\ 0 & 0 & 12 \end{bmatrix} \tag{51}$$

Dynamic decoupling allows the individual degrees of freedom to be controlled separately. Figure 13 shows the angular trajectories of the SEM, and Figure 14 represents the angular velocities of each direction.

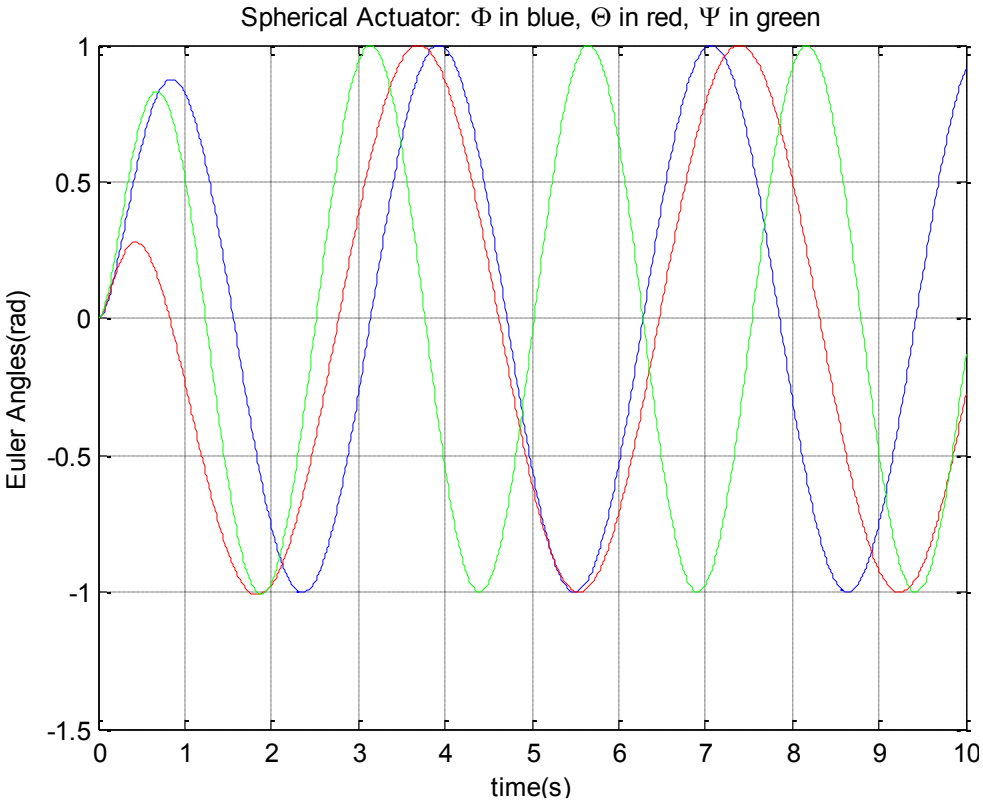

Figure 13: Angular Trajectories with Zero Initial Conditions

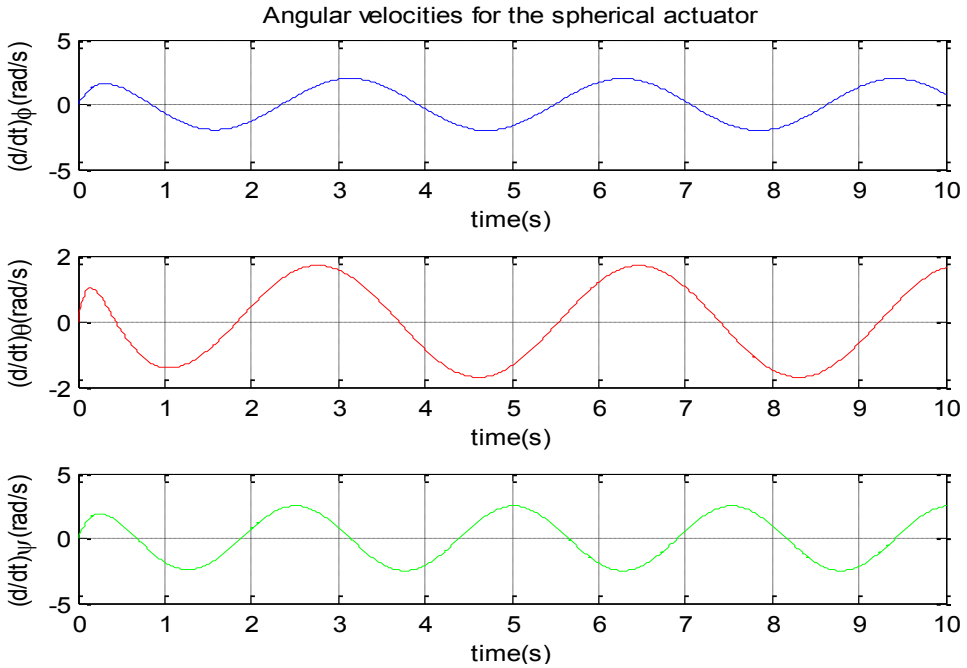

Figure 14: Angular Velocities with Zero initial Conditions

Figure 15 shows trajectory tracking. After several time trials, appropriate derivative and proportional constant K_d and K_p can be selected for the best tracking. The DDCTM algorithm achieves a good trajectory tracking performance by eliminating the inter-axis coupling and controlling each degree of freedom separately. Figure 16 shows the trajectory tracking error, which equals zero within third seconds. Figure 17 shows the input torque variation by time. Even though the high torque values present are based on desired trajectory, by adjusting K_d and K_p, input torque values can be calculated using the DDCTM algorithm.

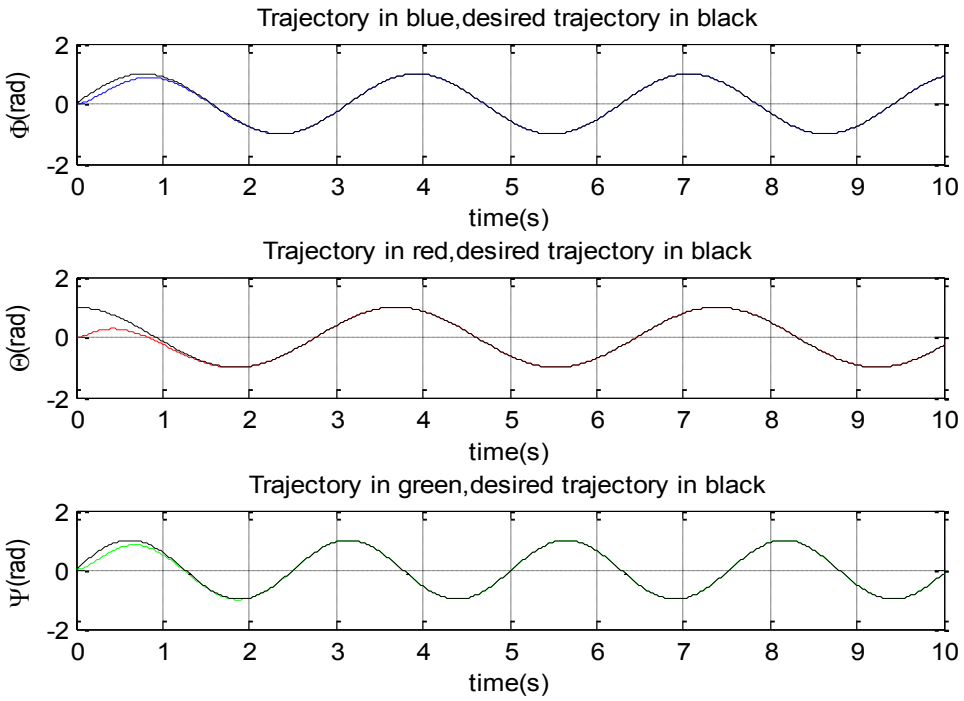

Figure 15: Trajectory Tracking with Zero Initial Conditions

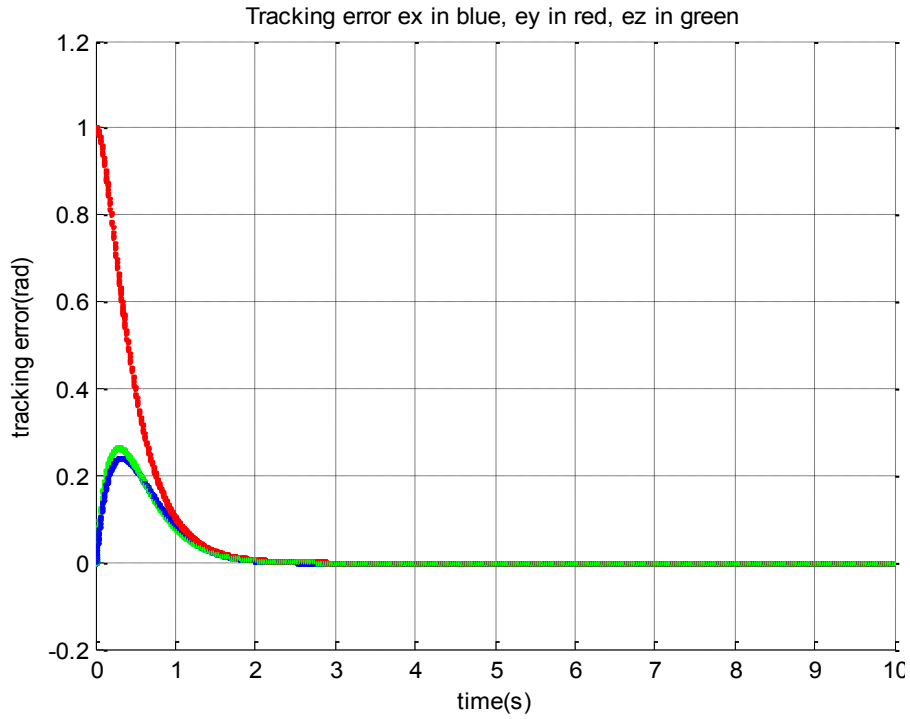

Figure 16: Trajectory Tracking Error with Zero Initial Conditions

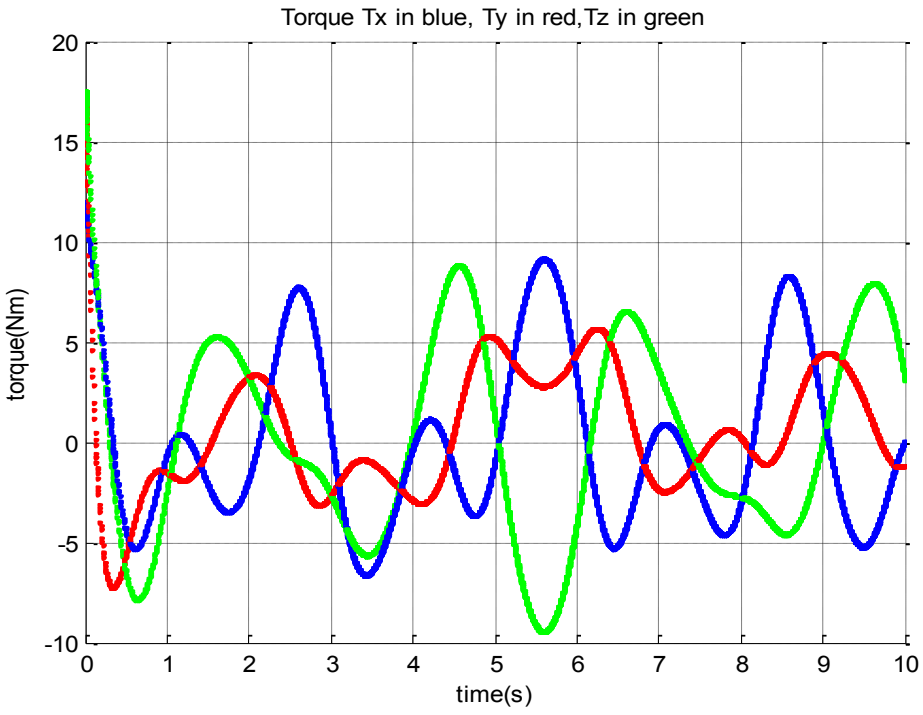

Figure 17: Input Torques with Zero Initial Conditions

Simulation with Non-Zero Initial Conditions

Let the initial conditions be as follows:

$$\theta = \begin{bmatrix} \phi \\ \theta \\ \psi \end{bmatrix} = \begin{bmatrix} 0.1 \\ 0.2 \\ 0.3 \end{bmatrix} \tag{52}$$

Using the same desired trajectory and controller constants would provide a good comparison between zero initial conditions trajectory tracking and non-zero initial conditions trajectory tracking:

$$\boldsymbol{\theta_d} = \begin{bmatrix} \sin(2t) \\ \cos(1.7t) \\ \sin(2.5t) \end{bmatrix}$$

The derivative and proportional controllers are set as diagonal matrices:

$$\boldsymbol{K_d} = \begin{bmatrix} 6 & 0 & 0 \\ 0 & 10 & 0 \\ 0 & 0 & 7 \end{bmatrix}$$

$$\boldsymbol{K_p} = \begin{bmatrix} 10 & 0 & 0 \\ 0 & 20 & 0 \\ 0 & 0 & 12 \end{bmatrix}$$

Figure 18 shows the angular trajectories of the SEM, Figure 19 shows the angular velocities, and Figure 20 shows the trajectory tracking. As can be seen in Figure 17, the DDCTM algorithm is still efficient with non-zero initial conditions. In Figure 21, trajectory tracking error is presented. Again, with non-zero initial conditions, the error is still reaching zero in a reasonable time. Figure 22 presents torque values by time.

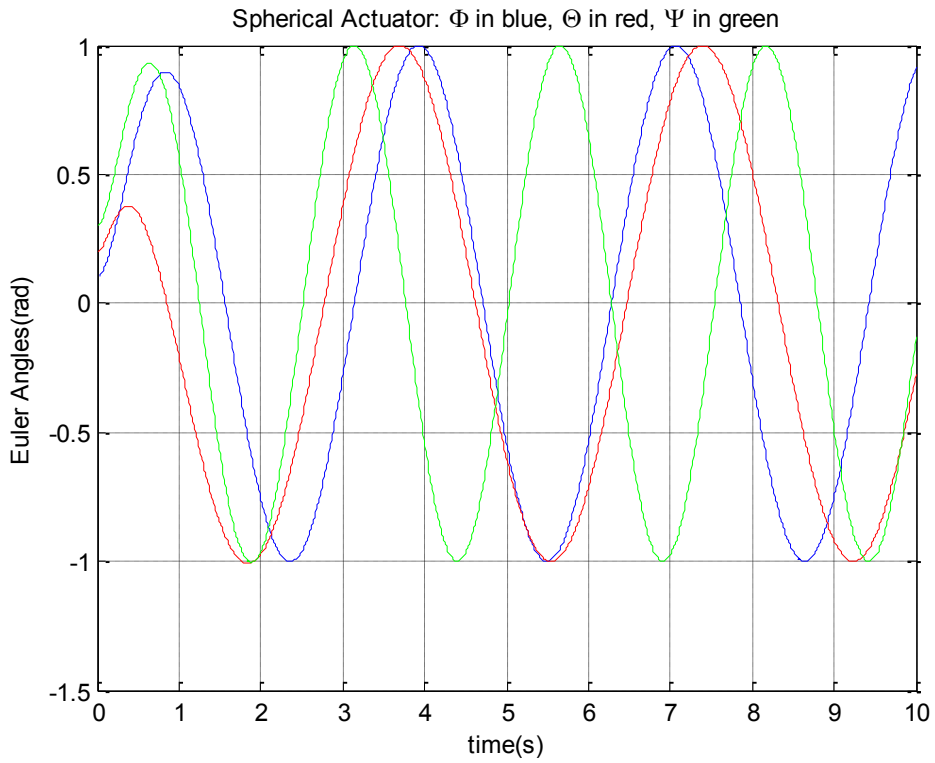

Figure 18: Angular Trajectories with Non-Zero Initial Conditions

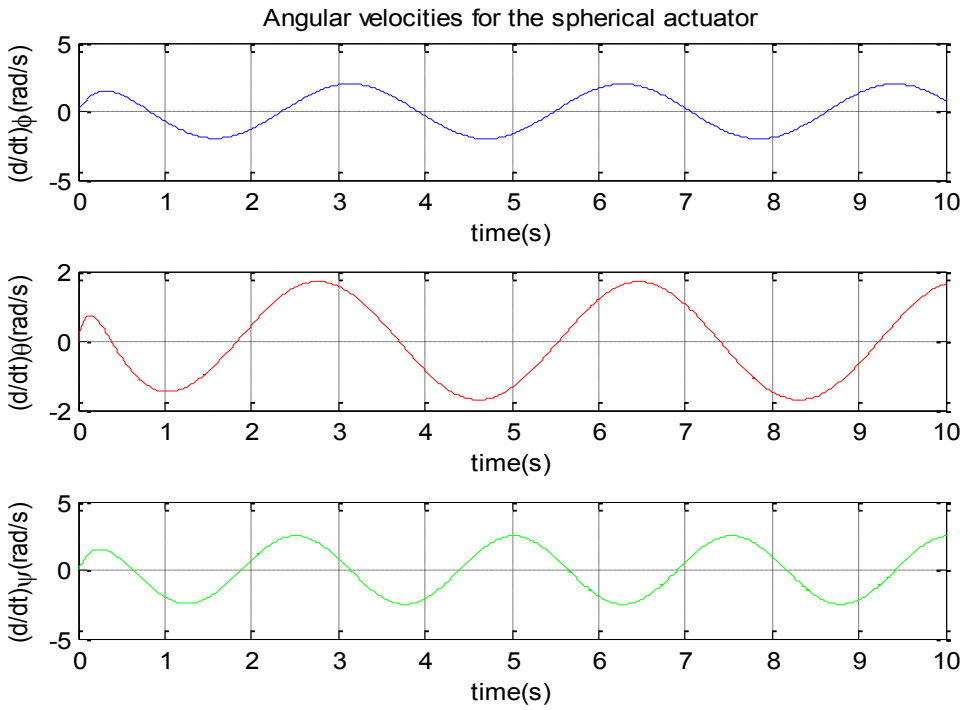

Figure 19: Angular Velocities with Non-Zero Initial Conditions

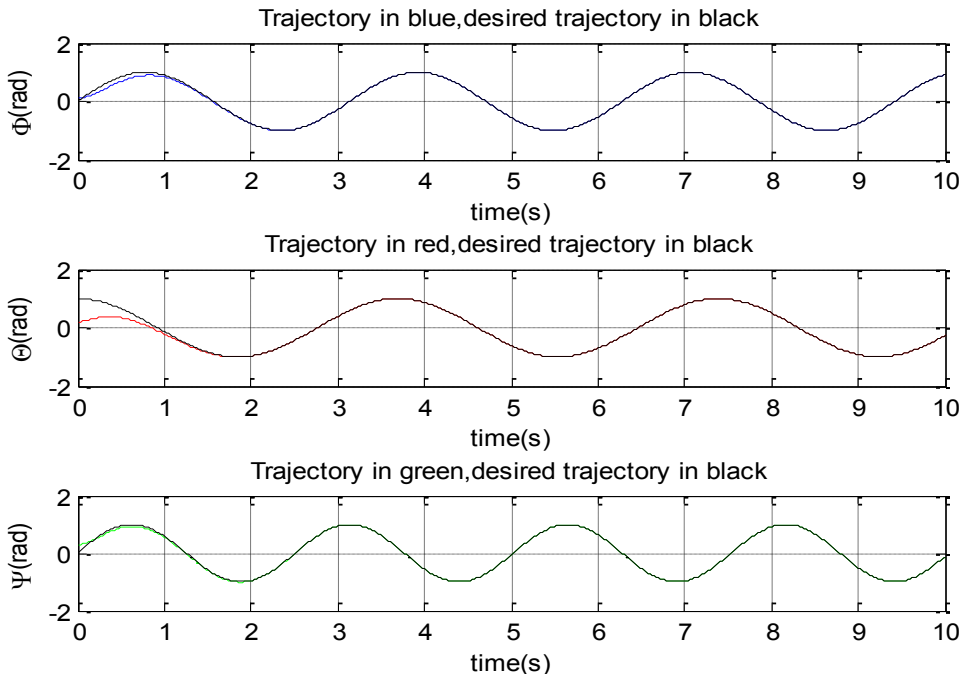

Figure 20: Trajectory Tracking with Non-Zero Initial Conditions

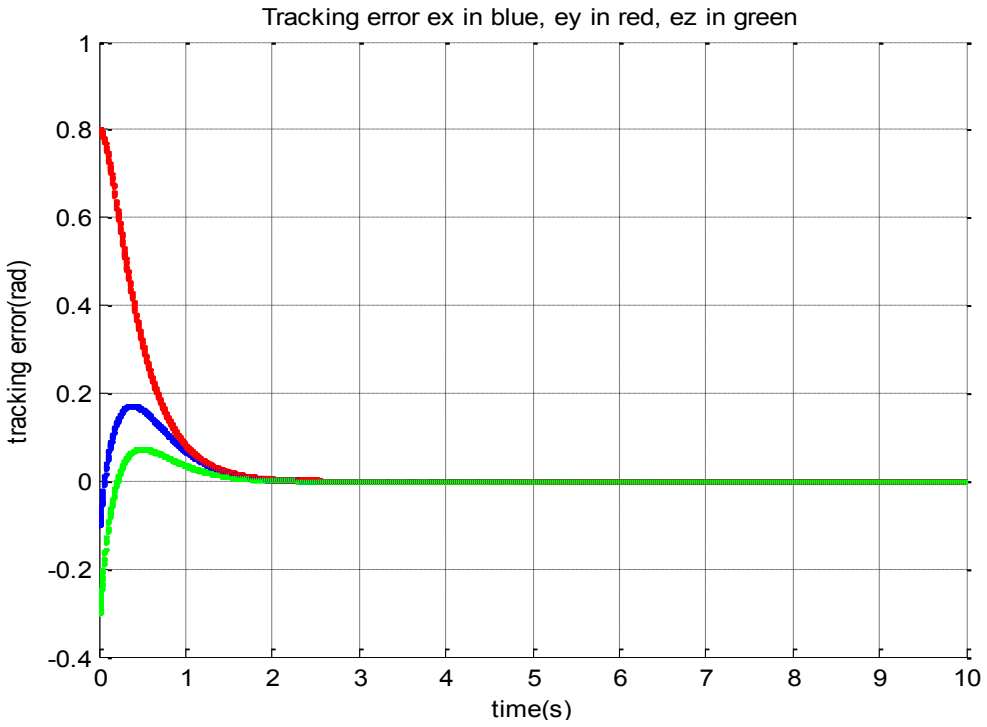

Figure 21: Trajectory Tracking Error with Non-Zero Initial Conditions

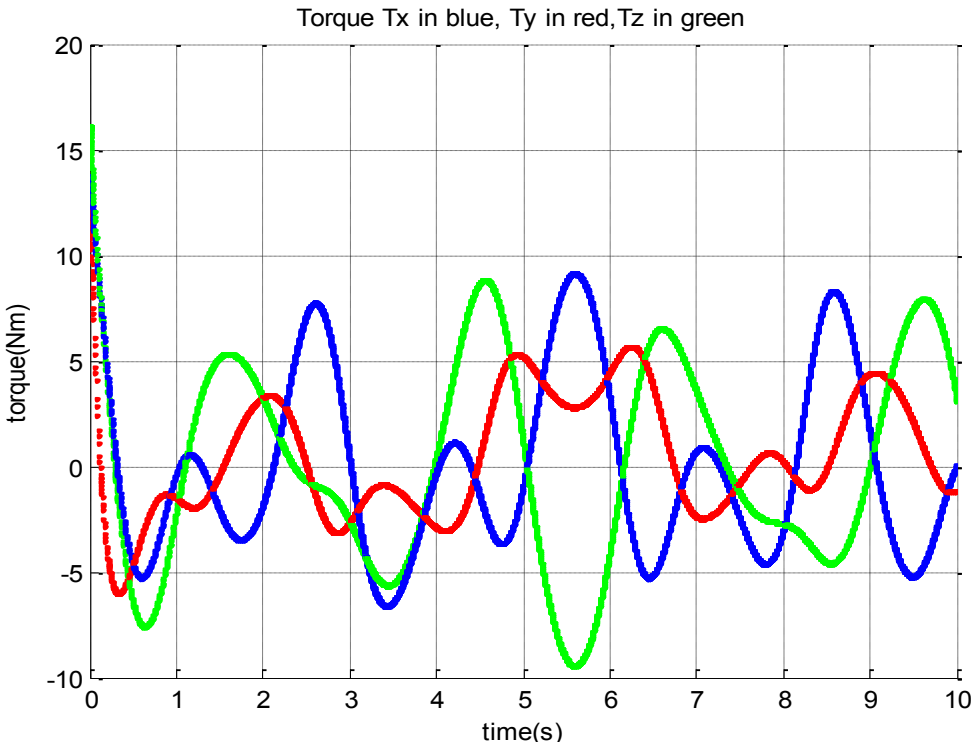

Figure 22: Input Torques with Non-Zero Initial Conditions

6.5. Conclusion

Using three-dimensional dynamics about a point, an SEM was modeled and controlled in a complex way. Nonlinear inter-axis coupling causes problems during position control. One of the most efficient algorithms for SEM control is the dynamic decoupling computed torque model. After the equation of motion is divided into inertial torque and Coriolis torque, each degree of freedom can be controlled separately. Good trajectory tracking in either the zero initial condition or non-zero initial condition proves the efficiency of the DDCTM algorithm.

CHAPTER 7

CONCLUSION AND FUTURE WORK

The aim of this research was to find good results for the industrial application of a spherical electric motor. Currently, the challenges in SEM research concern actuation, bearing system, and position control. In this research, a new actuation method was introduced. Especially at low speeds, precise position requirements, as in a robotic joint or electric car steering and suspension are satisfied by the new actuation method. This method is similar to that in LCD and magnetic suspension system procedures. With higher resolution of the controlled area comes the possibility of higher position accuracy, Nonlinear torque modeling was also derived. Finally, a nonlinear dynamic model of the proposed SEM was derived, and the DDCTM control algorithm was implemented. Simulation results have been shown for both zero initial conditions and non-zero initial conditions.

This research can be extended in many ways. In torque modeling, the torque function $f(\delta)$ needs to be calculated by either an experiment or finite element analysis for different applications. The proposed torque model is in a general form and can be applied in low-speed 2-DOF applications, like a robotic joint; low-speed 3-DOF applications, like an actuator or a robotic joint; and high-speed 3-DOF application, like an electric helicopter or morphing aircraft wing mechanisms. However, in high speed 3-DOF applications, the torque model needs a slight modification due to hybrid actuation methods. After a certain speed, rolling is generated by four moving poles on the stator by repulsion and attraction with four rotor poles (similar to a conventional stepper motor) because pitch and yaw are generated by the interaction of a single moving pole on the stator and south rotor pole.

The proposed SEM has many application areas. This research could also be extended by building prototypes for different applications. That would facilitate the procedure of commercializing SEM. Also, interaction with industry members of society about the SEM would help in getting it commercialized.

REFERENCES

REFERENCES

[1] Williams, F.C., Laithwaite, E.R., and Eastham, J.F., "Development and design of spherical induction motors," *Proceedings of IEEE—Part A: Power Engineering,* Vol. 106, No. 30, 1959, pp. 471–484.

[2] Davey, Kent, and Vachtsevanos, George, "On the control of a novel spherical robotic actuator," *Proceedings of 25th IEEE Conference on Decision and Control*, Vol. 25, Part: 1, 1986, pp. 415–416.

[3] Davey, K., Vachtsevanos, G., and Powers, R., "The analysis of fields and torques in spherical induction motors," *IEEE Transactions on Magnetics*, Vol. 23, No. 1, 1987, pp. 273–282.

[4] Miles, A.R., "Spherical electric motors," *IEEE Potentials*, Vol. 9, No. 3, 1990, pp. 47–48.

[5] Kaneko, K., Yamada, I., and Itao, K., "A spherical DC servo motor with three degrees of freedom," *ASME Dynamic Systems and Control*, Vol. 11, 1988, pp.433–443.

[6] Lee, K.-M., and Kwan, C.-K., "Design concept development of a spherical stepper for robotic applications," *IEEE Transactions on Robotics and Automation,* Vol. 7, No. 1, 1991, pp. 175–181.

[7] Chirikjian, G.S., and Stein, D., "Kinematic design and commutation of a spherical stepper motor," *IEEE/ASME Transactions on Mechatronics*, Vol. 4, No. 4, 1999, pp. 342–353.

[8] Byrns, E.V., Jr., Sweriduk, G.D., and Pettengill, J., "Low order robust dynamic compensation for a spherical wrist motor," *First IEEE Conference on Control Applications*, Vol. 1, 1992, pp. 258–263.

[9] Lee, Kok-Meng, and Wang, Xiao-an, "Dynamic modeling and control of a ball-joint-like variable-reluctance spherical motor," *Proceedings of IEEE American Control Conference*, 1992, pp. 2463–2467.

[10] Zhou, Zhi, and Lee, Kok-Meng, "Real-time motion control of a multi-degree-of-freedom variable reluctance spherical motor," *Proceedings of IEEE International Conference on Robotics and Automation*, Vol. 3, 1996, pp. 2859–2864.

[11] Toyama, S., Hatae, S., and Nonaka, M., "Development of multi-degree of freedom spherical ultrasonic motor," *Proceedings of IEEE Fifth International Conference on Advanced Robotics*, Vol. 1, 1991, pp. 55–60.

[12] Yano, T., Suzuki, T., Sonoda, M., and Kaneko, M., "Basic characteristics of the developed spherical stepping motor," *Proceedings of IEEE/RSJ International Conference on Intelligent Robots and Systems,* Vol. 3, 1999, pp. 1393–1398.

[13] Ezenekwe, D.E., and Kok-Meng Lee, "Design of air bearing system for fine motion application of multi-DOF spherical actuators," *Proceedings of IEEE/ASME International Conference on Advanced Intelligent Mechatronics,* 1999, pp. 812–818.

[14] Purwanto, E., and Toyama, S., "Control method of a spherical ultrasonic motor," *Proceedings of IEEE/ASME International Conference on Advanced Intelligent Mechatronics,* Vol. 2, 2003, pp. 1321–1326.

[15] Qian, Zhe, Wang, Qunjing, Ju, Lufeng, Wang, Anbang, and Liu, Jun, "Torque modeling and control algorithm of a permanent magnetic spherical motor," *Proceedings of International Conference on Electrical Machines and Systems,* 2009, pp. 1–6.

[16] Wu, Xingming, Guo, Fanghong, Chen, Weihai, and Liu, Jingmeng, "Design of open-loop controller for permanent magnet spherical motor," *Proceedings of 6th IEEE Conference on Industrial Electronics and Applications,* 2011, pp. 1122–1127.

[17] Li, Guoli, Li, Jiangjiang, Qian, Zhe, and Hu, Cungang, "Studies on position detection of permanent magnet spherical stepper motor based on machine vision," *Proceedings of International Conference on Electrical Machines and Systems*, 2008, pp. 1433–1436.

[18] Wang, Qunjing, Qian, Zhe, and Li, Guoli, "Vision based orientation detection method and control of a spherical motor," *Proceedings of 53rd IEEE International Midwest Symposium on Circuits and Systems,* 2010, pp.1145–1148.

[19] Wang, Qunjing, Li, Zheng, Chen, Lixia, and Xia, Kun, "The motion control algorithm and orientation detection methodology of a spherical stepper motor," *IEEE* International Conference on Information Acquisition, 2005.

[20] Dehez, B., Galary, G., Grenier, D., and Raucent, B., "Development of a spherical induction motor with two degrees of freedom," *IEEE Transactions on Magnetics,* Vol. 42, No. 8, 2006, pp. 2077–2089.

[21] Yan, Liang, Chen, I-Ming, Yang, Guilin, and Lee, Kok-Meng, "Analytical and experimental investigation on the magnetic field and torque of a permanent magnet spherical actuator," *IEEE/ASME Transactions on Mechatronics,* Vol. 11, No. 4, 2006, pp. 409–419.

[22] Wang, Qunjing, Li, Zheng, Ni, Youyuan, and Jiang, Weidong, "Magnetic field computation of a PM spherical stepper motor using integral equation method," *IEEE Transactions on Magnetics*, Vol. 42, No. 4, 2006 , pp. 731–734.

[23] Li, Zheng, and Wang, Qunjing, "Modeling and control of a permanent magnet spherical stepper motor," *Proceedings of International Conference on Electrical Machines and Systems,* 2007, pp. 1574–1579.

[24] Wang, Qunjing, and Xia, Kun, "Simulation of current control for a permanent magnet spherical stepper motor," *International Conference on Electrical Machines and Systems,* 2007, pp. 547–551.

[25] Li, Zheng, and Wang, Qun-Jing, "Neural network control schemes for PM spherical stepper motor drive," *Proceedings of International Conference on Machine Learning and Cybernetics*, Vol. 4, 2008, pp. 2042–2047.

[26] Li, Zheng, "Intelligent control for permanent magnet spherical stepper motor," *IEEE International Conference on Automation and Logistics,* 2008, pp. 1807–1812.

[27] Zheng Li, Wang, Qunjing, Bao, Xiaohua, and Xia, Kun, "Motion control algorithm and kinematic analysis of a spherical stepper motor," *Proceedings of Eighth International Conference on Electrical Machines and Systems*, Vol. 2, 2005, pp. 1659–1664.

[28] Ishikawa, M., and Kinouchi, Y., "Modeling and control of spherical ultrasonic motor based on nonholonomic mechanics," *Proceedings of International Conference on Intelligent Robots and Systems,* 2008, pp. 125–130.

[29] Li, Zheng, and Wang, Qunjing, "Robust neural network controller design for permanent magnet spherical stepper motor," *Proceedings of IEEE International Conference on Industrial Technology,* 2008, pp. 1–6.

[30] Lim, Chee Kian, Yan, Liang, Chen, I-Ming, Yang, Guilin, and Lin, Wei, "A novel approach in generating 3-DOF motion," *Proceedings of IEEE International Conference on Mechatronics and Automation*, Vol. 3, 2005, pp. 1485–1490.

[31] Li, Zheng, "Robust control of PM spherical stepper motor based on neural networks," *IEEE Transactions on Industrial Electronics*, Vol. 56, No. 8, 2009, pp. 2945–2954.

[32] Kun, Xia, Li-Xin, Ma, Wen-Tao, Fan, and Wang, Qun-Jing, "Design of the current controller for the permanent magnet spherical stepper motor," *Proceedings of International Conference on Electrical Machines and Systems*, 2009, pp. 1–4.

[33] Qian, Zhe, Wang, Qunjing, Ju, Lufeng, Wang, Anbang, and Liu, Jun, "Studies on vision based absolute orientation detection method of spherical motor," *Proceedings of International Conference on Electrical Machines and Systems*, 2009, pp. 1–6.

[34] Xia, Changliang, Guo, Chen, and Shi, Tingna, "A neural-network-identifier and fuzzy-controller-based algorithm for dynamic decoupling control of permanent-magnet spherical motor," *IEEE Transactions on Industrial Electronics,* Vol. 57, No. 8, 2010, pp. 2868–2878.

[35] Lee, Kok-Meng, and Son, Hungsun, "Torque model for design and control of a spherical wheel motor," *Proceedings of IEEE/ASME International Conference on Advanced Intelligent Mechatronics*, 2005, pp. 335–340.

[36] Mahto, M.K., Chitturi, A.B., Dehury, S., Sinha, S.K., and Chaturvedi, M., "Bipedal walking simulation with controlled vibration using MR fluid, electromagnetic dampers and spherical motors," *Proceedings of 2nd International Conference on Mechanical and Electrical Technology*, 2010, pp. 687–691.

[37] Son, Hungsun, and Lee, Kok-Meng, "Open-loop controller design and dynamic characteristics of a spherical wheel motor," *IEEE Transactions on Industrial electronics,* Vol. 57, No. 10, 2010, pp. 3475–3482.

[38] Zhang, Liang, Yan, Liang, Chen, Weihai, and Liu, Jingmeng, "Current optimization of 3-DOF permanent magnet spherical motor," *Proceedings of 6th IEEE Conference on Industrial Electronics and Applications*, 2011, pp. 1111–1116.

[39] Lim, Chee Kian, Yan, Liang, Chen, I-Ming, Yang, Guilin, and Lin, Wei, "Mechanical design & numerical electromagnetic analysis of a DC spherical actuator," *Proceedings of IEEE Conference on Robotics, Automation and Mechatronics*, Vol. 1, 2004, pp. 536–541.

[40] Wu, Xingming, Guo, Fanghong, Liu, Jingmeng, and Chen, Weihai, "Bounded control of a spherical actuator based on orientation measurement feedback," *Proceedings of IEEE International Conference on Robotics and Biomimetics*, 2011, pp. 727–732.

[41] Park, Hyun-Jong, Go, Sung-Chul, Lee, Ho-Joon and Lee, Ju, "D-Q-P vector control method with shaft response factor on 3-DOF 4 poles spherical PM motor, *Proceedings of IEEE International Symposium on Industrial Electronics*, 2012, pp. 623–628.

[42] Lee, Kok-Meng, and Sosseh, R.A., "Effects of fixture dynamics on back-stepping control of a VR spherical motor," *Proceedings of 7th International Conference on Control, Automation, Robotics and Vision*, 2002, pp. 384–389.

[43] Guo, Chen, and Xia, Changliang, "A dynamic decoupling control algorithm for Halbach array permanent magnet spherical motor based on computed torque method," *Proceedings of IEEE International Conference on Robotics and Biomimetics*, 2007, pp. 2090–2094.

[44] Moreno-Valenzuela, Javier, Santibáñez, Víctor, and Campa, Ricardo, "On output feedback tracking control of robot manipulators with bounded torque input," *International Journal of Control, Automation, and Systems*, Vol. 6, No. 1, 2008, pp. 76–85.

[45] Paden, Brad, and Panja, Ravi, "Globally asymptotically stable "PD+" controller for robot manipulators," *International Journal of Control*, Vol. 47, No. 6, 1988, pp. 1697–1712.

[46] Leea, Kok-Meng, Sosseh, Raye A., and Weia, Zhiyong, "Effects of the torque model on the control of a VR spherical motor," *Journal of Control Engineering Practice*, Vol. 12, No. 11, 2004, pp. 1437–1449.

[47] Meng, Yanyan, Chen, Weihai, Wang, Haihong, Liu, Jingmeng, and Wu, Xinming, "Closed-loop control of spherical actuator based on voltage model," *Proceedings of 7th IEEE Conference on Industrial Electronics and Applications*, 2012, pp. 319–323.

[48] Shan, Ximin, Kuo, Shih-Kang, Zhang, Jihua, and Menq, C.-H., "Ultra precision motion control of a multiple degrees of freedom magnetic suspension stage," *IEEE/ASME Transactions on Mechatronics*, 2002, Vol. 7, No. 1, pp. 67–78.

[49] Chan, S.H., and Nguyen, T.Q., "LCD Motion Blur: Modeling, analysis, and algorithm," *IEEE Transactions on Image Processing*, 2011, Vol. 20, No. 8, pp. 2352–2365.

[50] Huang, Shenghua, Wan, Shanming, and Fu, Guangjie, "Three-dimensional motor suitable for robotics and its decoupling control," *Proceedings of IEEE 22nd International Conference on Industrial Electronics, Control, and Instrumentation*, 1996, Vol. 3, pp. 1890–1895.

[51] Haiyan He, Janssen, J.G., and Bellers, E., "Low cost LCD panel frame rate doubling by applying Motion Controlled Dynamic Frame Insertion," *Digest of Technical Papers International Conference on Consumer Electronics*, 2009, pp. 1–2.

[52] Slotin J., and Li, W., *Applied Nonlinear Control*, Prentice Hall, 1991.

[53] Friedland, Bernard, *Control System Design,* McGraw-Hill, 1986.

[54] Yan, L., Chen, I-Ming, Lim, C. K., Yang, G., and Lee, Kok-Meng, *Design, Modeling and Experiments of 3-DOF Electromagnetic Spherical Actuators*, Springer, 2011.

APPENDIX

APPENDIX

DYNAMICALLY DECOUPLING COMPUTED TORQUE PROGRAM

SphericalElectricMotor.m

```
% Function of Spherical Electric Motor recieves initial conditions for
% motion angles,derivative of motion angles,torque,and tracking errors and
% final time as inputs. The function calls function Sphere to get
% derivatives of motion angles, speeds, torques, and tracking errors.
% Spherical Electric Motor returns working trajectories of the
% spherical motor by time and solution of the differential equations in
% Xderivative by ode23
function [t,X] = SphericalElectricMotor(x0,tf)
t0=0;
tspan=linspace(t0,tf,1000);
[t,X]=ode23('Sphere',tspan,x0);
% SPHERICAL ELECTRIC MOTOR TRAJECTORIES
% Rotor Shaft Position
Phi= X(:,1); Theta=X(:,2); Psi=X(:,3);
% DESIRED SPHERICAL ELECTRIC MOTOR TRAJECTORIES
% Desired Rotor Position
Phid = sin(2*t); Thetad = cos(1.7*t); Psid = sin(2.5*t);

figure(1)
plot(t,X(:,1),'b',t,X(:,2),'r',t,X(:,3),'g'), grid on
ylabel('Euler Angles(rad)'),xlabel('time(s)')
title('Spherical Actuator: \Phi in blue, \Theta in red, \Psi in green')
hold on
```

```
figure(2)
subplot(3,1,1),plot(t,X(:,4),'b'), grid on
ylabel('(d/dt)\phi(rad/s)'),xlabel('time(s)')
title('Angular velocities for the spherical actuator')
subplot(3,1,2),plot(t,X(:,5),'r'), grid on
ylabel('(d/dt)\theta(rad/s)'),xlabel('time(s)')
subplot(3,1,3),plot(t,X(:,6),'g'), grid on
ylabel('(d/dt)\psi(rad/s)'),xlabel('time(s)')
hold on

figure(3)
subplot(3,1,1),plot(t,Phi,'b',t,Phid,'k'), grid on
title(' Trajectory in blue,desired trajectory in black '),ylabel('\Phi(rad)'),xlabel('time(s)'),
subplot(3,1,2),plot(t,Theta,'r',t,Thetad,'k'), grid on
title('Trajectory in red,desired trajectory in black'),ylabel('\Theta(rad)'),xlabel('time(s)')
subplot(3,1,3),plot(t,Psi,'g',t,Psid,'k'), grid on
title('Trajectory in green,desired trajectory in black'),ylabel('\Psi(rad)'),xlabel('time(s)')
hold on

figure(4)
title('Tracking error ex in blue, ey in red, ez in green')
xlabel('time(s)'),ylabel('tracking error(rad)'), grid on
```

```
figure(5)
title('Torque Tx in blue, Ty in red,Tz in green')
xlabel('time(s)'),ylabel('torque(Nm)'),grid on
```

Sphere.m

```
function Xderivative = Sphere(t,X)
% Controller matrices:
kp=[10 0 0;0 20 0;0 0 12]; kd=[6 0 0;0 10 0;0 0 7];
% DESIRED TRAJECTORY
Phid = sin(2*t); Thetad = cos(1.7*t); Psid = sin(2.5*t);
% DESIRED ANGULAR SPEEDS
dPhid = 2*cos(2*t); dThetad = -1.7*sin(1.7*t); dPsid = 2.5*cos(2.5*t);
% DESIRED ANGULAR ACCELERATIONS
ddPhid= -4*sin(2*t); ddThetad= -2.89*cos(1.7*t); ddPsid= -6.25*sin(2.5*t);
% COMPUTED-TORQUE CONTROLLER
% TRACKING ANGULAR ERRORS:
ex = Phid-X(1); ey = Thetad-X(2); ez = Psid-X(3);
% TRACKING ANGULAR SPEED ERRORS
dex = dPhid-X(4); dey = dThetad-X(5); dez = dPsid-X(6);
figure(4)
hold on
plot(t,ex,'b',t,ey,'r',t,ez,'g'),grid on
% M(q,qdot) Moment of inertia matrix
m11= 1; m12= 0; m13= sin(X(2)); m21= 0; m22= 1; m23= 0; m31= sin(X(2)); m32= 0; m33= 1;
```

```
% C(q,qdot) Coriolis matrix
C=[0,X(6)*cos(X(2)),0;-X(6)*cos(X(2)),0,0;X(5)*cos(X(2)),0,0];
% CONTROL TORQUES
t1 = ddPhid + kd(1,1)*dex + kp(1,1)*ex;
t2 = ddThetad + kd(2,2)*dey + kp(2,2)*ey;
t3 = ddPsid + kd(3,3)*dez + kp(3,3)*ez;
T1 = m11*t1 + m12*t2 + m13*t3 + C(1,1)*X(4)+C(1,2)*X(5)+C(1,3)*X(6);
T2 = m21*t1 + m22*t2 + m23*t3 + C(2,1)*X(4)+C(2,2)*X(5)+C(2,3)*X(6);
T3 = m31*t1 + m32*t2 + m33*t3 + C(3,1)*X(4)+C(3,2)*X(5)+C(3,3)*X(6);
figure(5)
hold on
plot(t,T1,'b',t,T2,'r',t,T3,'g'),grid on
% DYNAMICS OF SPHERICAL ELECTRIC MOTOR:
M=[m11 m12 m13; m21 m22 m23;m31 m32 m33];
IM= inv(M);
Xderivative=[X(4);
    X(5);
    X(6);
    IM(1,1)*(T1-X(6)*cos(X(2))*X(5))+IM(1,2)*(T2+X(6)*cos(X(2))*X(4))+IM(1,3)*(T3-
X(5)*cos(X(2))*X(4));
    IM(2,1)*(T1-X(6)*cos(X(2))*X(5))+IM(2,2)*(T2+X(6)*cos(X(2))*X(4))+IM(2,3)*(T3-
X(5)*cos(X(2))*X(4));
    IM(3,1)*(T1-X(6)*cos(X(2))*X(5))+IM(3,2)*(T2+X(6)*cos(X(2))*X(4))+IM(3,3)*(T3-
X(5)*cos(X(2))*X(4));
```

```
(T1-X(7))/(.01);
(T2-X(8))/(.01);
(T3-X(9))/(.01);
(ex-X(10))/(.01);
(ey-X(11))/(.01);
(ez-X(12))/(.01)];
```